

Effect of gas-transfer-velocity parameterization choice on CO₂ air-sea fluxes in the North Atlantic and the European Arctic

Iwona Wrobel^{1,2} and Jacek Piskozub^{1,2}

¹ IOPAS - Centre for Polar Studies KNOW (Leading National Research Centre), Sopot, Poland

² Institute of Oceanology, Polish Academy of Sciences, Sopot, Poland

Correspondence to: I. Wróbel (iwrobel@iopan.gda.pl)

Abstract

The ocean sink is an important part of the global carbon budget. Because the terrestrial biosphere is usually treated as a residual, understanding the uncertainties in the net flux into the ocean is crucial for understanding the global carbon cycle. One of the sources of uncertainty is the parameterization for the CO₂ gas transfer velocity. We used a recently developed software tool, FluxEngine, in order to estimate monthly net carbon air-sea flux for the extratropical North Atlantic, the European Arctic, as well as global values (for comparison) using several available parameterizations of the gas transfer velocity for different dependence on wind speed, both quadratic and cubic. The aim of the study is to constrain the uncertainty caused by the choice of parameterization in the North Atlantic, a large sink of CO₂ and a region with good measurement coverage, characterized by strong winds. We show that this uncertainty is smaller in the North Atlantic and in the Arctic than globally, within 5% in the North Atlantic and 4% in the European Arctic, comparing to 9% for the World Ocean when restricted to functions with quadratic wind dependence and respectively 42%, 40% and 67% for all studied parameterizations. We propose an explanation of this smaller uncertainty caused by combination of higher than global average wind speeds in the North Atlantic and lack of seasonal changes in the flux direction in most of the region. We also compare the available *p*CO₂ climatologies (Takahashi and SOCAT), *p*CO₂ discrepancy in annual flux values of 8% in the North Atlantic and 19% in the European Arctic. The seasonal flux changes in the Arctic have inverse seasonal change in both climatologies, caused most probably by insufficient data coverage, especially in winter.

1. Introduction

The region of extratropical North Atlantic, including the European Arctic, is a region where a large part of ocean deep waters are formed (see Talley (2013) for a recent review). This process, part of the global overturning circulation, makes the area a large sink of CO₂ (Takahashi et al. 2002; Takahashi et al., 2009; Landschützer et al., 2014; Le Quéré et al., 2015), including its anthropogenic fraction (Orr et al. 2001). Therefore, there is a widespread interest in tracing the changes in North Atlantic carbon fluxes, especially as models predict a decrease in the sink volume later in this century (Halloran et al., 2015).

The trends in North Atlantic CO₂ sink has been intensively studied since observations showed it is decreasing (Lefevre et al. 2004). The sink decrease on interannual time scales has been confirmed by further studies (Schuster and Watson, 2007) and continued in recent years north of 40° N (Landschützer et al., 2013). It is not certain how much of this change is due to long-term changes, how much to decadal changes in atmospheric forcing, namely the North Atlantic Oscillation (Gonzalez-Davila et al., 2007; Thomas et al., 2008; Gruber 2009; Watson et al., 2009) and changes in meridional overturning circulations (Perez et al., 2013). Recent assessments of the Atlantic and

52 Arctic sea–air CO₂ fluxes (Schuster et al., 2013) and global ocean carbon uptake (Wanninkhof et al.,
53 2013) showed that this problem has not been yet resolved.

54
55 Studying the volume of the ocean CO₂ sink and especially its trends, one needs to constrain the flux
56 uncertainty. Its sources are sampling coverage, methods of data interpolation, in-water fugacity data
57 quality, the method used for normalization of fugacity data to a reference year in a world of ever
58 increasing atmospheric CO₂ partial pressure and the choice of gas transfer velocity k
59 parameterization (Landschützer et al., 2014; Woolf et al., 2015a, 2015b). In this work we chose to
60 analyze various empirical parametrization using wind speed. Although the North Atlantic is one of
61 the regions of the world ocean best covered by CO₂ fugacity measurements (Watson et al., 2011),
62 the Arctic seas coverage is much poorer, especially in winter (Schuster et al., 2013).

63
64 One of the factors influencing the value of calculated air-sea gas flux is the choice of formula for
65 gas transfer velocity. Literature of the subject has several parameterizations to choose from with
66 different dependence on wind speed (cubic or quadratic). This problem is not trivial as indicated
67 even by the name of one of the meetings on the topic the COST-735 Action organized “ k
68 conundrum” workshop (in Norwich, February 2008). Its results have been incorporated into a recent
69 review book chapter (Garbe et al., 2014). This paper will concentrate on the very uncertainty caused
70 by the choice of gas flux velocity parameterization in the case of the North Atlantic and the
71 European Arctic. The region was chosen due to being the area of many studies some of the
72 parameterizations were based on and also as a region with wind distribution tilted to higher winds
73 than the global average to test the effect of stronger winds on the difference of net fluxes calculated
74 using the published gas transfer velocity formulas.

75

76

77 2. Methods

78

79 2.1 Datasets

80

81 We calculated air-sea carbon dioxide fluxes using a set of processing tools named ‘FluxEngine’
82 (Shutler et al., 2016) (which is available on the <http://www.ifremer.fr/cersat/exp/oceanflux/>),
83 created within European Space Agency founded OceanFlux Greenhouse Gases project (Goddijn-
84 Murphy et al., 2015). All calculations were performed using the FluxEngine software, we were only
85 end-users of. The software is scheduled to be opening sourced but at the time of this study we did
86 not have more information about it than is included in the paper describing the tool set (Shutler et
87 al., 2016). This was a conscious decision because, even as we had access to the toolset developers,
88 we wanted to test it as end users (this is probably the first study using the toolset by authors who
89 had no part in creating it). The idea beyond the tool development has been to encourage the use of
90 satellite Earth Observation (EO) data for studying air-sea fluxes. Within the FluxEngine, a suite of
91 reanalyzes, *in situ* and model data are available as input to the toolbox that can be use by the
92 scientific community and to aid the interpretation of the resultant flux data. There is a choice of
93 several different flux parameterizations as well as input data allowing the generation of monthly
94 global gridded flux products with 1°x1° spatial resolution. The output files contained twelve sets
95 (one set per month) in a NetCDF files. Each data set includes the mean (first order moment),
96 median, standard deviation and the second, third and fourth order moments calculated for each
97 calendar month. There is also information about origin of data inputs as well as results of our
98 calculated. Input data users can chose from all available on the FluxEngine program (perhaps from
99 monthly EO data: rain intensity and event, wind speed and direction, % of ice age and thickness,
100 from monthly model data ECMWF air pressure, whitecapping, from monthly climatology as $p\text{CO}_2$,
101 SST, salinity) and configurable them in a various way. The user needs to choose different
102 components in a calculation process as a way of computed transfer velocity, parametrization to the

103 wind speed calculation, corrections etc. The FluxEngine has been developed not only to support the
104 study of the air-sea flux of CO₂ but also to aid the study of other gases as DMS and N₂O (Land et
105 al., 2013; Shutler et al., 2016).

106
107 For the calculations, we used $p\text{CO}_2$ and salinity values from Takahashi et al. (2009) climatology
108 based on more than 3 million measurements of surface water $p\text{CO}_2$ in open-ocean environments
109 during non El Nino conditions (recalculated to fugacity in the FluxEngine toolset). For some
110 calculations we used, as an alternative, Surface Ocean CO₂ Atlas (SOCAT) ver. 1.5 and 2.0 (Sabine
111 et al., 2013; Pfeil et al., 2013; Bakker and al., 2014) $p\text{CO}_2$ and SST data. SOCAT is a community
112 driven dataset containing respectively 6.3 and 10.1 million surface water CO₂ fugacity values with a
113 global coverage. Both climatologies were calculated for year 2010 within the FluxEngine toolset.
114 The SST values were taken from Operational Sea Surface Temperature and Sea Ice Analysis
115 (OSTIA) (Donlon et al., 2011), and in the SOCAT case from the database, while SST skin data we
116 used came from ARC/(A)ATSR Global Monthly Sea Surface dataset (Merchant et al., 2012). Both
117 data sets have been preprocessed in the same way using the toolsets of FluxEngine (Shutler et al.,
118 2016).

119
120 We used Earth Observation (EO) wind speed and sea roughness (σ_0 in Ku band from GlobWave
121 L2P products) data obtained from the European Space Agency (ESA) Environmental monitoring
122 satellite, Envisat. Envisat was launched in 2002 with 10 instruments onboard into sun-synchronous
123 near-polar orbit (SSO) with 35 day repeat cycle. It carries, among others, two atmospheric sensors
124 monitoring trace gases. EO data supports earth science research and allows monitoring of the
125 evolution of environmental and climate change.

126
127 All the data were used globally within the FluxEngine software. From the gridded product (1 x 1
128 deg) we extracted extratropical North Atlantic (North of 30° N), and its subset, the European Arctic
129 (North of 64° N).

130 131 2.2. k parameterizations

132
133 The flux of CO₂ at the interface of air and the sea is controlled by wind speed, sea state, sea
134 surface temperature (SST) and other factors. We estimate the air-sea flux of CO₂ (OF , g C m⁻²
135 day⁻¹) as the product of gas transfer velocity (k , ms⁻¹) and also the difference in CO₂ concentration
136 (gm⁻³) at the sea water and the interface – air (Land et al., 2013). The concentration of CO₂ in sea
137 water is a product of its solubility (α , gm⁻³ μatm) and its fugacity ($f\text{CO}_2$, μatm). Solubility is, in
138 turn, a function of salinity and temperature. Hence Eq. (1) is represented as:

$$139 \quad F = k (\alpha_W f\text{CO}_{2W} - \alpha_S f\text{CO}_{2A}) \quad (1)$$

140
141
142 where the subscripts denote values in water (W) and the air-sea interface (S) and in the air (A). We
143 can exchange fugacity to the partial pressure (their values differ by <0.5 % over the temperature
144 range considered) (McGillis et al., 2001). So equation (2) now becomes:

$$145 \quad F = k (\alpha_W p\text{CO}_{2W} - \alpha_S p\text{CO}_{2A}) \quad (2)$$

146
147
148 We can also ignore the differences between the two solubilities and just use the water side
149 solubility α_W . Equation (3) will be represented as:

$$150 \quad F = k \alpha_W (p\text{CO}_{2W} - p\text{CO}_{2A}) \quad (3)$$

151
152
153 This formulation is often referred to the ‘bulk parametrization’.

154
155
156
157
158
159
160
161
162
163
164
165
166
167
168
169
170
171
172

In this work we chose to analyze the fluxes using five different parameterizations, within the FluxEngine software, using in terms of wind speed to parametrized k . All of them are parameterized with wind speed and differ in the formula for gas transfer velocity, k :

$$k = \sqrt{(660.0 / Sc_{skin}) * (0.212 U_{10}^2 + 0.318 U_{10})} \quad (4)$$

(Nightingale et al., 2000),

$$k = \sqrt{(660.0 / Sc_{skin}) * 0.254 U_{10}^2} \quad (5)$$

(Ho et al., 2006),

$$k = \sqrt{(660.0 / Sc_{skin}) * 0.0283 U_{10}^3} \quad (6)$$

(Wanninkhof and McGillis, 1999),

$$k = \sqrt{(660.0 / Sc_{skin}) * 0.251 U_{10}^2} \quad (7)$$

(Wanninkhof, 2014),

$$k = \sqrt{(660.0 / Sc_{skin}) * (3.3 + 0.026 U_{10}^3)} \quad (8)$$

(McGillis et al., 2001),

173
174
175
176
177
178

where the subscripts are Schmidt numbers at the skin surface (Sc_{skin}), a function of SST ($[=$ (kinematic viscosity of water)/(diffusion coefficient of CO_2 in water], 660.0 is the Schmidt number for carbon dioxide at 20 °C temperature in seawater, U_{10} is the wind speed 10 m above the sea surface.

179
180
181
182
183
184
185
186
187

In addition to the purely wind driven parameterizations, we have used a combined Goddijn-Murphy et al. (2012) and Fangohr and Woolf (2007) parametrization, created as part of OceanFlux GHG project and provided as an option in FluxEngine. This parameterization separates contributions from direct and bubble-mediated gas transfer as suggested by Woolf (2005). Its purpose is to enable separate evaluation of the effect of the two processes on gas fluxes and should be not treated as a final product (one of the aims of the ongoing OceanFlux Evolution project is improving this parameterization). We used these OceanFluxGHG parameterizations in two versions: wind driven (using the U_{10} wind fields) and radar backscatter driven (using mean wave square slope) as described in Goddijn-Murphy et al. (2012).

188
189
190

3. Results

191
192
193
194
195
196
197
198
199
200
201
202
203

Using the FluxEngine software, we have produced CO_2 global monthly gridded air-sea fluxes and calculated from them the values for the study region, extratropical North Atlantic and separately for its subset, the European Arctic seas. Figure 1 shows maps of average CO_2 fluxes for North Atlantic, calculated with Nightingale et al. 2000 (named further as N2000) k formula and Takahashi (2009) climatology for the whole year and for each season. The area as a whole is a carbon sink but even the all-season map shows that some regions close to North Atlantic Drift and East Greenland Current are net sources. The seasonal maps show even more variability. For example the above mentioned sinks areas become sinks in summer (effect of phytoplankton blooms) while the southernmost areas of the study become CO_2 sources in summer and autumn (effect of sea-water temperature changes). Much of this variability is caused by changes of the surface water pCO_2 average values, shown in Figure 2 for the whole year and for each season (and variability in atmospheric CO_2 partial pressure, not shown). However, the flux is proportional to the product of

204 $\Delta p\text{CO}_2$ and k . In most parameterizations k is a function of wind speed (eqs. 4-8). The average wind
205 speed U_{10} for the whole year and each season is shown in Figure 3. The wind speeds in the North
206 Atlantic are higher than the mean in the world ocean, with average values higher than 10 m s^{-1}
207 in many regions of the study area in all seasons except the summer (with highest values in winter).
208 This is important because the fluxes depend not only on average wind speed but also on its
209 distribution (see also the Discussion). This effect is especially visible between formulas with
210 different powers of U_{10} . Figure 4 shows the difference in calculated fluxes on the example of two
211 parameterizations: one proportional to U_{10}^3 (eq. 6) and one to U_{10}^2 (eq. 7), namely Wanninkhof and
212 McGillis (1999) and Wanninkhof (2014). It can be seen that the “cubic” function results in higher
213 absolute flux values, comparing to a “quadratic” one, in regions of high winds and lower with
214 weaker winds.

215
216 Figure 5 shows the monthly values of CO_2 fluxes for the five parameterizations (eq. 4-8) for the
217 North Atlantic and the European Arctic. The areas are a sink in every month, although August is
218 close to neutral for the North Atlantic. The results using two cubic formula (eqs. 6 and 8) are higher
219 in absolute values respectively by 30% for Wanninkhof and McGillis (1999) and 55% for McGillis
220 (2001), comparing to “quadratic” N2000 (eq. 4). The other two “quadratic” parameterizations (eqs.
221 5 and 7) resulted in fluxes within 5% of N2000. Annual fluxes for the North Atlantic and the
222 European Arctic and global (for comparison) are shown in Figure 6. In addition to the five
223 parameterizations, the figure presents results for both the OceanFluxGHG formulas (using wind and
224 radar backscatter data). The mean and standard deviations of the parametrization ensemble are
225 shown as gray vertical lines. The uncertainty in global fluxes is similar to previous estimates
226 (Sweeney et al., 2007, Landschützer et al., 2014) but they cannot be directly compared due to
227 different parameterization choices and methodologies. Annual North Atlantic flux, depending on
228 the formula used, varies from -0.38 TgC for N2000 to -0.56 TgC for McGillis et al. (2001). In the
229 case of global carbon flux the values are, respectively, -1.30 TgC and -2.15 TgC . Figure 7 shows the
230 same data “normalized” to N2000, the parameterization resulting in lower absolute flux values, to
231 visualize the relative differences. In the case of the North Atlantic, using the “quadratic”
232 Wanninkhof (2014) and Ho et al. (2006) results in a flux respectively 3% and 5% higher in absolute
233 value than N2000, while the “cubic” Wanninkhof and McGillis (1999) and McGillis et al. (2001)
234 results in respectively 28% and 42% higher values. The respective values for the Arctic are 3%, 4%
235 for quadratic as well as 27% and 40% for cubic functions. In the case of global flux the respective
236 values are 8% and 9% higher than N2000 flux for the quadratic functions as well as 34% and 67%
237 for cubic ones. The OceanFluxGHG parameterization results in fluxes 18% and 32% higher for
238 North Atlantic than N2000 (for respectively backscatter and wind driven versions). In the case of
239 global values this surplus was, respectively, 45% and 52%.

240
241 All the above results used the Takahashi (2009) $p\text{CO}_2$ climatology. For comparison we have also
242 calculated fluxes using SOCAT version 1.5 and 2.0, interpolated to create a climatology using the
243 FluxEngine toolset (Shutler et al., 2016). Figure 8 shows the results using N2000 k parameterization
244 for all the three climatologies. In the case of the North Atlantic study area, although the monthly
245 values show large differences (both SOCAT climatologies result in larger sink in summer and
246 smaller in winter comparing to Takahashi), the annual values are similar: -0.38 TgC for both
247 Takahashi and SOCAT v.1.5 and -0.41 TgC for SOCAT v. 2.0. In the case of the European Arctic
248 the situation is different, with Takahashi and SOCAT climatologies resulting in inverse seasonal
249 variability even as annual flux results are similar: -0.102 TgC for Takahashi, -0.085 TgC for
250 SOCAT v. 1.5 and -0.088 TgC for SOCAT v. 2.0.

251

252

253 4. Discussion

254

255 Our result show that using the three “quadratic” parameterizations (Nightingale et al., 2000; Ho et
 256 al., 2006 and Wanninkhof 2014) results in fluxes values within 5% of each other in the case of
 257 North Atlantic. This discrepancy is smaller than the 9% difference for the net global carbon air-sea
 258 flux (Fig. 7). This would confirm that, at present, the parameterizations are interchangeable being
 259 all within the experimental uncertainty. This view was supported by the leading authors of the three
 260 parameterizations during a discussion session convened by them (Nightingale, 2015) during
 261 SOLAS Open Science Conference in Kiel, Germany on 7-11 September 2015). The three
 262 parameterizations were derived using different methods and data from different regions, namely
 263 passive tracers and dual-trace experiments in the North Sea in the case of Nightingale et al. (2000),
 264 dual tracers in the Southern Ocean in the case of Ho et al. (2006) and global ocean ¹⁴C inventories
 265 in the case of Wanninkhof (2014). This makes it possible to be highly confident that at least average
 266 fluxes calculated with the three formulas are close to the unknown true values. However, the
 267 uncertainties are still large and although the quadratic functions are supported by several lines of
 268 evidence (see Garbe et. al., 2014 for discussion), other powers are not completely refuted by the
 269 available observations. Therefore it is important to notice that a choice of one of the available cubic
 270 functions may lead to net fluxes larger in absolute values up to 33% in the North Atlantic and 50%
 271 globally.

272
 273 The above results imply smaller relative differences between the parameterizations in North
 274 Atlantic than globally. This is interesting because North Atlantic is a region of strong winds and in
 275 most of its area no seasonal changes in the flux direction (Fig. 1). This is even more surprising if
 276 one realizes that, at least some of the older parameterizations were developed basing on smaller
 277 wind ranges than the ones present in the North Atlantic. After analysing this unexpected fact using
 278 the formula multiplied by different wind distribution, we have found two reasons for that. First,
 279 when comparing quadratic and cubic parameterizations (Fig. 9), it is clear that cubic ones imply
 280 higher fluxes for high winds while quadratic one for weak winds. This difference can be presented
 281 in arithmetic terms. Let us assume two functions of wind speed U , $F_1(U)$ quadratic and $F_2(U)$ cubic:

$$282 \quad F_1(U) = a U^2, \quad (9)$$

$$283 \quad F_2(U) = b U^3. \quad (10)$$

284
 285
 286
 287 The difference between the two functions ΔF is equal to

$$288 \quad \Delta F = F_2 - F_1 = b U^3 - a U^2 = b U^2 (U - a b^{-1}) = b U^2 (U - U_x) \quad (11)$$

289
 290 where $U_x = a b^{-1}$. The difference is positive for wind speeds greater than U_x and negative for smaller
 291 ones. U_x is the value of wind speed for which the two functions intersect. In the case of equations
 292 (6) and (7), $a = 0.251$ and $b = 0.0283$, implying $U_x = 8.87 \text{ m s}^{-1}$. In fact all the functions presented in
 293 Fig. 9 have very similar values for wind speeds close to 9 m s^{-1} . The value is very close to average
 294 wind speeds in the North Atlantic (Fig. 3). This is one of the reasons of small relative net flux
 295 differences. The other is lack of seasonality. In case of seasonal changes in the flux direction
 296 (caused by seasonal changes in water temperature or primary productivity), with winds stronger
 297 than U_x in some seasons and weaker in other (usually strong winds in winter and weak in summer),
 298 the fluxes partly cancel each other while the difference between cubic and quadratic
 299 parameterizations add to each other due to simultaneous changes in the sign of both fluxes itself and
 300 the $U - U_x$ term. This effect of seasonality has been suggested to us basing on available data (A.
 301 Watson – personal communication) but we are unaware of any paper explaining it in the terms of
 302 arithmetic formulas, or even describing it explicitly.

303
 304
 305 In addition to the five parameterizations described above, we calculated fluxes for the

306 OceanFluxGHG combined formula, separating contributions from direct and bubble-mediated gas
307 transfer. The resultant fluxes are higher, in absolute terms, from all the quadratic functions
308 considered in this study, being closer to cubic ones. This may mean that the bubble mediated term
309 of Fangohr and Woolf (2007) may be an overestimation for CO₂ fluxes. This question will be the
310 subject of further studies in the OceanFlux Evolution project.

311
312 Although using both the Takahashi and SOCAT *p*CO₂ climatologies (Fig. 8) results in similar
313 annual fluxes in the North Atlantic, it should be noted that they show different seasonal changes.
314 This may have been caused by slightly different time periods of the climatologies (SOCAT is more
315 recent). The difference is much larger in the European Arctic due to much worse data spatial
316 coverage and possible interpolation artifacts (Goddijn-Murphy et al., 2015). This discrepancy
317 makes us treat the flux results from the Arctic with much less confidence than the ones for the
318 whole North Atlantic. This situation may improve after SOCAT v.3 which is planned to be released
319 in 2016.

320 321 322 5. Conclusions

323
324 In this paper we have studied the effect of choice of gas transfer velocity parameterization on the
325 net CO₂ air-sea gas flux volume in the North Atlantic and European Arctic using the recently
326 developed FluxEngine software. The results show that the uncertainty caused by the choice of the *k*
327 formula is smaller in the North Atlantic and in the Arctic than globally. The annual net flux
328 difference caused by the choice of parameterization is within 5% in the North Atlantic and 4% in
329 the European Arctic, comparing to 9% globally for the studied functions with quadratic wind
330 dependence and respectively 42% for North Atlantic, 40% for Arctic and 67% between the cubic
331 and quadratic functions. We explain the smaller North Atlantic variability by the combination of
332 higher than global average wind speeds in the North Atlantic, closer to 9 m s⁻¹, the wind speed when
333 most *k* parameterization have similar values and the all-season CO₂ sink conditions in most North
334 Atlantic areas. We compare the Takahashi and SOCAT *p*CO₂ climatologies finding that although the
335 seasonal variability in the North Atlantic is different, annual net fluxes are within 8% in the North
336 Atlantic and 19% in the European Arctic. The seasonal flux changes in the Arctic have inverse
337 seasonal change in both climatologies indicating possible under sampling and therefore the need for
338 more polar *p*CO₂ data before than available at present.

339 340 341 342 Acknowledgements

343
344 The publication has been financed from the funds of the Leading National Research Centre
345 (KNOW) received by the Centre for Polar Studies for the period 2014-2018; OceanFlux
346 Greenhouse Gases Evolution, a project funded by the European Space Agency, ESRIN Contract No.
347 4000112091/14/I-LG; and GAME "Growing of Marine Arctic Ecosystem", funded by Narodowe
348 Centrum Nauki grant DEC-2012/04/A/NZ8/00661.

349 350 351 352 353 354 References

355
356 Bakker, D. C. E., Pfeil, B., Smith, K., Hankin, S., Olsen, A., Alin, S. R., Cosca, C., Harasawa, S.,

- 357 Kozyr, A., Nojiri, Y., O'Brien, K. M., Schuster, U., Telszewski, M., Tilbrook, B., Wada, C., Akl,
358 J., Barbero, L., Bates, N. R., Boutin, J., Bozec, Y., Cai, W.-J., Castle, R. D., Chavez, F. P., Chen,
359 L., Chierici, M., Currie, K., de Baar, H. J. W., Evans, W., Feely, R. A., Fransson, A., Gao, Z.,
360 Hales, B., Hardman-Mountford, N. J., Hoppema, M., Huang, W.-J., Hunt, C. W., Huss, B.,
361 Ichikawa, T., Johannessen, T., Jones, E. M., Jones, S. D., Jutterström, S., Kitidis, V., Körtzinger,
362 A., Landschützer, P., Lauvset, S. K., Lefevre, N., Manke, A. B., Mathis, J. T., Merlivat, L., Metzl,
363 N., Murata, A., Newberger, T., Omar, A. M., Ono, T., Park, G.-H., Paterson, K., Pierrot, D., Ríos,
364 A. F., Sabine, C. L., Saito, S., Salisbury, J., Sarma, V. V. S. S., Schlitzer, R., Sieger, R., Skjelvan,
365 I., Steinhoff, T., Sullivan, K. F., Sun, H., Sutton, A. J., Suzuki, T., Sweeney, C., Takahashi, T.,
366 Tjiputra, J., Tsurushima, N., van Heuven, S. M. A. C., Vandemark, D., Vlahos, P., Wallace, D. W.
367 R., Wanninkhof, R., and Watson, A. J.: An update to the Surface Ocean CO₂ Atlas (SOCAT
368 version 2), *Earth Syst. Sci. Data*, 6, 69-90, doi:10.5194/essd-6-69-2014, 2014.
- 369
- 370 Donlon, C. J., Martin, M., Stark, J. D., Roberts-Jones, J., Fiedler, E., and Wimmer, W.: The
371 Operational Sea Surface Temperature and Sea Ice Analysis (OSTIA), *Remote Sens. Environ.*,
372 Special Issue 116, 140-158, doi: 10.1016/j.rse.2010.10.017, 2011.
- 373
- 374 Fangohr, S. and Woolf, D. K.: Application of new parameterizations of gas transfer velocity and
375 their impact on regional and global CO₂ budgets, *J. Marine Syst.*, 66, 195-203, 2007.
- 376
- 377 Garbe, C. S., Rutgersson, A., Boutin, J., de Leeuw, G., Delille, B., Fairall, C. W., Gruber, N., Hare,
378 J., Ho, D. T., Johnson, M. T., Nightingale, P. D., Pettersson, H., Piskozub, J., Sahlee, E., Tsai, W.,
379 Ward, B., Woolf, D. K., and Zappa, C. J.: Transfer Across the Air-Sea Interface, in: *Ocean-
380 Atmosphere Interactions of Gases and Particles*, edited by: Liss, P. S. and Johnson, M. T.,
381 Springer, Earth System Science, Springer, Berlin, Heidelberg, 55–111, 2014.
- 382
- 383 Goddijn-Murphy, L. M., Woolf, D. K., and Marandino, C.: Space-based retrievals of air-sea gas
384 transfer velocities using altimeters: Calibration for dimethyl sulfide, *J. Geophys. Res.*, 117,
385 C08028, doi: 10.1029/2011JC007535, 2012.
- 386
- 387 Goddijn-Murphy, L. M., Woolf, D. K., Land, P. E., Shutler J. D., Donlon, C.: The OceanGlux
388 Greenhouse Gases methodology for deriving a sea surface climatology of CO₂ fugacity in
389 support of air-sea gas lux studies, *Ocean Sci.*, 11, 519-541, 2015, doi: 10.5194/os-11-519-2015,
390 2015.
- 391
- 392 Gonzalez-Davila, M., Santana-Casiano, J. M., and Gonzalez-Davila, E. F.: Interannual variability of
393 the upper ocean carbon cycle in the northeast Atlantic Ocean, *Geophys. Res. Lett.*, 34, L07608,
394 doi: 10.1029/2006GL028145, 2007.
- 395
- 396 Gruber, N.: Fickle trends in the ocean, *Nature*, 458, 155-156, doi: 10.1038/458155a, 2009.
- 397
- 398 Halloran, P. R., Booth, B. B. B., Jones, C. D., Lambert, F. H., McNeall, D. J., Totterdell, I. J., and
399 Völke, C.: The mechanisms of North Atlantic CO₂ uptake in a large Earth System Model
400 ensemble, *Biogeosciences*, 12, 4497–4508, doi: 10.5194/bg-12-4497-2015, 2015.
- 401
- 402 Ho, D., Law C., Smith M., Schlosser P., Harvey M., Hill P.: Measurements of air-sea gas exchange
403 at high wind speeds in the Southern Ocean: Implications for global parametrizations, *Geophys.
404 Res. Lett.*, 33, L16611, doi: 10.1029/2006/GL026817, 2006.
- 405
- 406 Landschützer, P., Gruber, N., Bakker, D. C. E., Schuster, U., Nakaoka, S., Payne, M. R., Sasse, T. P.,
407 and Zeng, J.: A neural network-based estimate of the seasonal to inter-annual variability of the

408 Atlantic Ocean carbon sink, *Biogeosciences*, 10, 7793-7815, doi: 10.5194/bg-10-7793-2013,
409 2013.

410

411 Landschützer, P., Gruber, N., Bakker, D. C. E., Schuster, U.: Recent variability of the global ocean
412 carbon sink, *Global Biogeochem. Cy.*, 28, 927–949, doi: 10.1002/2014GB004853, 2014.

413

414 Le Quéré, C., Moriarty, R., Andrew, R. M., Peters, G. P., Ciais, P., Friedlingstein, P., Jones, S. D.,
415 Sitch, S., Tans, P., Arneeth, A., Boden, T. A., Bopp, L., Bozec, Y., Canadell, J. G., Chini, L. P.,
416 Chevallier, F., Cosca, C. E., Harris, I., Hoppema, M., Houghton, R. A., House, J. I., Jain, A. K.,
417 Johannessen, T., Kato, E., Keeling, R. F., Kitidis, V., Klein Goldewijk, K., Koven, C., Landa, C.
418 S., Landschützer, P., Lenton, A., Lima, I. D., Marland, G., Mathis, J. T., Metzl, N., Nojiri, Y.,
419 Olsen, A., Ono, T., Peng, S., Peters, W., Pfeil, B., Poulter, B., Raupach, M. R., Regnier, P.,
420 Rödenbeck, C., Saito, S., Salisbury, J. E., Schuster, U., Schwinger, J., Séférian, R., Segschneider,
421 J., Steinhoff, T., Stocker, B. D., Sutton, A. J., Takahashi, T., Tilbrook, B., van der Werf, G. R.,
422 Viovy, N., Wang, Y.-P., Wanninkhof, R., Wiltshire, A., and Zeng, N.: Global carbon budget 2014,
423 *Earth Syst. Sci. Data*, 7, 47–85, doi: 10.5194/essd-7-47-2015, 2015.

424

425 Lefevre, N., Watson, A. J., Olsen, A., Rios, A. F., Perez, F. F., Johannessen, T.: A decrease in the
426 sink for atmospheric CO₂ in the North Atlantic, *Geophys. Res. Lett.*, 31, L07306, doi:
427 10.1029/2003GL018957, 2004.

428

429 McGillis, W. R., and Edson, J. B., Hare, J. E., Fairall, C. W.: Direct covariance air-sea CO₂ fluxes,
430 *J. Geophys. Res.*, 106, 729-16, 2001.

431

432 Merchant, C. J., Embury, O., Rayner, N. A., Berry, D. I., Corlett, G. K., K., L., Veal, K. L., Kent, E.
433 C., T., L.-J. D., Remedios, J. J., and Saunders, R.: A 20 year independent record of sea surface
434 temperature for climate from Along-Track Scanning Radiometers, *J. Geophys. Res.*, 117, 2012.

435

436 Nightingale, P. D., Malin, G., Law, C. S., Watson, A. J., Liss, P. S., Liddicoat, M. I., Boutin, J., and
437 Upstill-Goddard, R. C.: In situ evaluation of air-sea gas exchange parametrizations using novel
438 conservative and volatile tracers, *Global Biogeochem. Cy.*, 14, 373-387, 2000.

439

440 Nightingale, P. D., Relationship between wind speed and gas exchange over the ocean: which
441 parameterisation should I use?, Raport from Discussion Session at SOLAS Open Science
442 conference in Kiel, <http://goo.gl/TrMQkg>, 2015.

443

444 Orr, J. C., Maier-Reimer, E., Mikolajewicz, U., Monfray, P., Sarmiento, J. L., Toggweiler, J. R.,
445 Taylor, N. K., Palmer, J., Gruber, N., Sabine, C. L., Quéré, C. Le., Key, R. M., Boutin, J.:
446 Estimates of anthropogenic carbon uptake from four three-dimensional global ocean models,
447 *Global Biogeochem. Cy.*, 15(1), 43-60, doi: 10.1029/2000GB001273, 2001.

448

449 Pérez, F. F., Herlé Mercier, Marcos Vázquez-Rodríguez, Pascale Lherminier, Anton Velo,
450 Paula C. Pardo, Gabriel Rosón and Aida F. Ríos: Atlantic Ocean CO₂ uptake reduced by
451 weakening of the meridional overturning circulation, *Nat. Geosci.*, 6, 146-152, doi:
452 10.1038/NNGEO1680, 2013.

453

454 Pfeil, B., Olsen, A., Bakker, D. C. E., Hankin, S., Koyuk, H., Kozyr, A., Malczyk, J., Manke, A.,
455 Metzl, N., Sabine, C. L., Akl, J., Alin, S. R., Bates, N., Bellerby, R. G. J., Borges, A., Boutin, J.,
456 Brown, P. J., Cai, W.-J., Chavez, F. P., Chen, A., Cosca, C., Fassbender, A. J., Feely, R. A.,
457 González-Dávila, M., Goyet, C., Hales, B., Hardman-Mountford, N., Heinze, C., Hood, M.,
458 Hoppema, M., Hunt, C. W., Hydes, D., Ishii, M., Johannessen, T., Jones, S. D., Key, R. M.,

459 Körtzinger, A., Landschützer, P., Lauvset, S. K., Lefevre, N., Lenton, A., Lourantou, A.,
460 Merlivat, L., Midorikawa, T., Mintrop, L., Miyazaki, C., Murata, A., Nakadate, A., Nakano, Y.,
461 Nakaoka, S., Nojiri, Y., Omar, A. M., Padin, X. A., Park, G.-H., Paterson, K., Perez, F. F., Pierrot,
462 D., Poisson, A., Ríos, A. F., Santana-Casiano, J. M., Salisbury, J., Sarma, V. V. S. S., Schlitzer,
463 R., Schneider, B., Schuster, U., Sieger, R., Skjelvan, I., Steinhoff, T., Suzuki, T., Takahashi, T.,
464 Tedesco, K., Telszewski, M., Thomas, H., Tilbrook, B., Tjiputra, J., Vandemark, D., Veness, T.,
465 Wanninkhof, R., Watson, A. J., Weiss, R., Wong, C. S., and Yoshikawa-Inoue, H.: A uniform,
466 quality controlled Surface Ocean CO₂ Atlas (SOCAT), *Earth Syst. Sci. Data*, 5, 125-143, doi:
467 10.5194/essd-5-125-2013, 2013.

468

469 Sabine, C. L., Hankin, S., Koyuk, H., Bakker, D. C. E., Pfeil, B., Olsen, A., Metzl, N., Kozyr, A.,
470 Fassbender, A., Manke, A., Malczyk, J., Akl, J., Alin, S. R., Bellerby, R. G. J., Borges, A.,
471 Boutin, J., Brown, P. J., Cai, W.-J., Chavez, F. P., Chen, A., Cosca, C., Feely, R. A., González-
472 Dávila, M., Goyet, C., Hardman-Mountford, N., Heinze, C., Hoppema, M., Hunt, C. W., Hydes,
473 D., Ishii, M., Johannessen, T., Key, R. M., Körtzinger, A., Landschützer, P., Lauvset, S. K.,
474 Lefevre, N., Lenton, A., Lourantou, A., Merlivat, L., Midorikawa, T., Mintrop, L., Miyazaki, C.,
475 Murata, A., Nakadate, A., Nakano, Y., Nakaoka, S., Nojiri, Y., Omar, A. M., Padin, X. A., Park,
476 G.-H., Paterson, K., Perez, F. F., Pierrot, D., Poisson, A., Ríos, A. F., Salisbury, J., Santana-
477 Casiano, J. M., Sarma, V. V. S. S., Schlitzer, R., Schneider, B., Schuster, U., Sieger, R., Skjelvan,
478 I., Steinhoff, T., Suzuki, T., Takahashi, T., Tedesco, K., Telszewski, M., Thomas, H., Tilbrook, B.,
479 Vandemark, D., Veness, T., Watson, A. J., Weiss, R., Wong, C. S., and Yoshikawa-Inoue, H.:
480 Surface Ocean CO₂ Atlas (SOCAT) gridded data products, *Earth Syst. Sci. Data*, 5, 145-153, doi:
481 10.5194/essd-5-145-2013, 2013.

482

483 Schuster, U., and Watson, A. J.: A variable and decreasing sink for atmospheric CO₂ in the North
484 Atlantic, *J. Geophys. Res.*, 112, C11006, doi: 10.1029/2006JC003941, 2007.

485

486 Schuster, U., McKinley, G. A., Bates, N., Chevallier, F., Doney, S. C., Fay, A. R., Gonzalez-Davila,
487 M., Gruber, N., Jones, S., Krijnen, J., Landschützer, P., Lefevre, N., Manizza, M., Mathis, J.,
488 Metzl, N., Olsen, A., Rios, A. F., Rodenbeck, C., Santana-Casiano, J. M., Takahashi, T.,
489 Wanninkhof, R., and Watson, A. J.: An assessment of the Atlantic and Arctic sea-air CO₂ fluxes,
490 1990–2009, *Biogeosciences*, 10, 607–627, doi: 10.5194/bg-10-607-2013, 2013.

491

492 Shutler, J. D., Piolle, J-F., Land, P. E., Woolf, D. K., Goddijn-Murphy, L., Paul, F., Girard-Ardhuin,
493 F., Chapron, B., and Donlon, C. J.: FluxEngine: a flexible processing system for calculating air-
494 sea carbon dioxide gas fluxes and climatologies, *J. Atmos. Ocean. Tech.*,
495 <http://dx.doi.org/10.1175/JTECH-D-14-00204.1>, 2016.

496

497 Sweeney, C., Gloor, E., Jacobson, A. R., Key, R. M., McKinley, G., Sarmiento, J. L. and
498 Wanninkhof, R.: Constraining global air-sea gas exchange for CO₂ with recent bomb 14C
499 measurements, *Global Biogeochem. Cycles*, 21, GB2015,
500 <http://dx.doi.org/10.1029/2006GB002784>, 2007.

501

502 Takahashi, T., Sutherland, S. G., Sweeney, C., Poisson, A. P., Metzl, N., Tilbrook, B., Bates, N. R.,
503 Wanninkhof, R., Feely, R. A., Sabine, C. L., Olafsson, J., and Nojiri, Y.: Global sea-air CO₂ flux
504 based on climatological surface ocean pCO₂, and seasonal biological and temperature effects,
505 *Deep Sea Res., Pt. II*, 49, 1601-1622, 2002.

506

507 Takahashi, T., Sutherland, S. C., Wanninkhof, R., Sweeney, C., Feely, R. A., Chipman, D. W., Hales,
508 B., Friederich, G., Chavez, F., Sabine, C., Watson, A., Bakker, D. C. E., Schuster, U., Metzl, N.,
509 Inoue, H. Y., Ishii, M., Midorikawa, T., Nojiri, Y., Koertzinger, A., Steinhoff, T., Hoppema, M.,

510 Olafsson, J., Arnarson, T. S., Tilbrook, B., Johannessen, T., Olsen, A., Bellerby, R., Wong, C. S.,
511 Delille, B., Bates, N. R., and de Baar, H. J. W.: Climatological mean and decadal change in
512 surface ocean $p\text{CO}_2$ and net sea-air CO_2 flux over the global oceans, *Deep-Sea Res. Pt. II*, 56,
513 554–577, doi: 10.1016/j.dsr2.2008.12.009, 2009.

514

515 Talley, L. D.: Closure of the Global Overturning Circulation Through the Indian, Pacific, and
516 Southern Oceans: Schematics and Transports, *Oceanography* 26(1), 80–97,
517 doi:10.5670/oceanog.2013.07, 2013.

518

519 Thomas, H., Friederike Prowe, A. E., Lima, I. D., Doney, S. C., Wanninkhof, R., Greatbatch, R. J.,
520 Schuster, U., and Corbiere, A.: Changes in the North Atlantic Oscillation influence CO_2 uptake
521 in the North Atlantic over the past 2 decades, *Global Biogeochem. Cy.*, 22, GB4027,
522 doi:10.1029/2007GB003167, 2008.

523

524 Wanninkhof, R.: Relationship between wind speed and gas exchange over the ocean revisited,
525 *Limnol. Oceanogr.- Meth.*, 12, 351–362, 2014.

526

527 Wanninkhof, R., and McGillis, W. R.: A cubic relationship between air-sea CO_2 exchange and wind
528 speed, *Geophys. Res. Lett.*, 26, 1889–1892, 1999.

529

530 Wanninkhof, R., Park, G.-H., Takahashi, T., Sweeney, C., Feely, R., Nojiri, Y., Gruber, N., Doney,
531 S. C., McKinley, G. A., Lenton, A., Quéré C. Le, Heinze, C., Schwinger, J., Graven, H.,
532 Khatiwala, S.: Global ocean carbon uptake: magnitude, variability and trends, *Biogeosciences*,
533 10, 1987–2013, doi: 10.5194/bg-10-1987-2013, 2013.

534

535 Watson, A. J., Schuster, U., Bakker, D. C. E., Bates, N. R., Corbière, A., González-Dávila, M.,
536 Friedrich, T., Hauck, J., Heinze, C., Johannessen, T., Körtzinger, A., Metzl, N., Olafsson, J.,
537 Olsen, A., Oschlies, A., Padin, X.A., Pfeil, B., Santana-Casiano, J.M., Steinhoff, T., Telszewski,
538 M., Rios, A.F., Wallace, D.W., Wanninkhof, R.: Tracking the variable North Atlantic sink for
539 atmospheric CO_2 , *Science*, 326(5958), 1391–1393, doi: 10.1126/science.1177394, 2009.

540

541 Watson, A. J., Metzl, N., Schuster, U.: Monitoring and interpreting the ocean uptake of atmospheric
542 CO_2 , *Philos. T. R. Soc. A*, 369, 1997–2008, doi: 10.1098/rsta.2011.0060, 2011.

543

544 Woolf, D. K.: Parameterization of gas transfer velocities and sea-state dependent wave breaking.
545 *Tellus B*, 57, 87–94, 2005.

546

547 Woolf, D. K., Shutler, J. D., Goddijn-Murphy, L., Donlon, C. J., Nightingale, P. D., Land, P. E.,
548 Torres, R., Chapron, B., Piolle, J-F., Herledan, S., Hanafin, J., Girard-Ardhuin, F., Ardhuin, F.,
549 Prytherch, J., Moat, B., and Yelland, M.: Key uncertainties in the contemporary air-sea flux of
550 carbon dioxide: an OceanFlux study, submitted 2015a.

551

552 Woolf, D. K., Goddijn-Murphy, L. M., Shutler, J. D., Land, P. E., Donlon, C. J., Prytherch, J.,
553 Yelland, M. J., Nightingale, P. D., Torres, R., Chapron, B., Piolle, J-F., Herledan, S., Hanafin, J.,
554 Girard-Ardhuin, F., Ardhuin F., and Moat, B.: Sources and types of uncertainty in the
555 contemporary air-sea flux of carbon dioxide: an OceanFlux study, submitted 2015b.

556

557 Figure 1. Seasonal and annual mean air-sea fluxes of CO₂ (mg C m⁻² day⁻¹) in the North Atlantic,
558 combine using Nightingale et al. (2000) *k* parameterization and Takahashi (2009) climatology in a)
559 annual, b) DJF (Winter), c) MAM (Spring), d) JJA (Summer), e) SON (Autumn). The gaps (white
560 areas) are due to missing data, land and ice masks and interpolation algorithms of the FluxEngine
561 software.

562

563 Figure 2. Seasonal and annual *p*CO₂ values (µatm) in surface waters of the North Atlantic,
564 estimated using Takahashi (2009) climatology in a) annual, b) DJF (Winter), c) MAM (Spring), d)
565 JJA (Summer), e) SON (Autumn). The gaps (white areas) are due to missing data, land and ice
566 masks and interpolation algorithms of the FluxEngine software.

567

568 Figure 3. Wind speed distribution *U*₁₀ (ms⁻²) in the North Atlantic used to determine the
569 relationship between gas transfer velocity and air-sea CO₂ fluxes in a) annual, b) DJF (Winter), c)
570 MAM (Spring), d) JJA (Summer), e) SON (Autumn). The gaps (white areas) are due to missing
571 data, land and ice masks and interpolation algorithms of the FluxEngine software.

572

573 Figure 4. Differences maps for the air-sea CO₂ fluxes (mg C m⁻² day⁻¹) in the North Atlantic,
574 between a wind cubed and squared parameterizations (Wanninkhof and McGillis 1999 and
575 Wanninkhof 2014) in a) annual, b) DJF (Winter), c) MAM (Spring), d) JJA (Summer) e) SON
576 (Autumn). The gaps (white areas) are due to missing data, land and ice masks and interpolation
577 algorithms of the FluxEngine software.

578

579 Figure 5. Monthly values air-sea fluxes of CO₂ (Tg/month) for the five parameterizations (eq. 4-8)
580 in a) North Atlantic, b) European Arctic.

581

582 Figure 6. Annual air-sea fluxes of CO₂ (Tg/year) for the five (eq. 4-8) parameterizations as well as
583 for backscatter (default) and wind driven OceanFluxGHG parameterization (see text) in a) global, b)
584 North Atlantic c) European Arctic. Average values for all parameterization and standard deviations
585 are marked as vertical gray lines.

586

587 Figure 7. Annual air-sea fluxes of CO₂ (Tg/year) for the five (eq. 4-8) parameterizations as well as
588 for backscatter (default) and wind driven OceanFluxGHG parameterization normalized to flux
589 values of Nightingale et al. (2000) *k* parameterization.

590

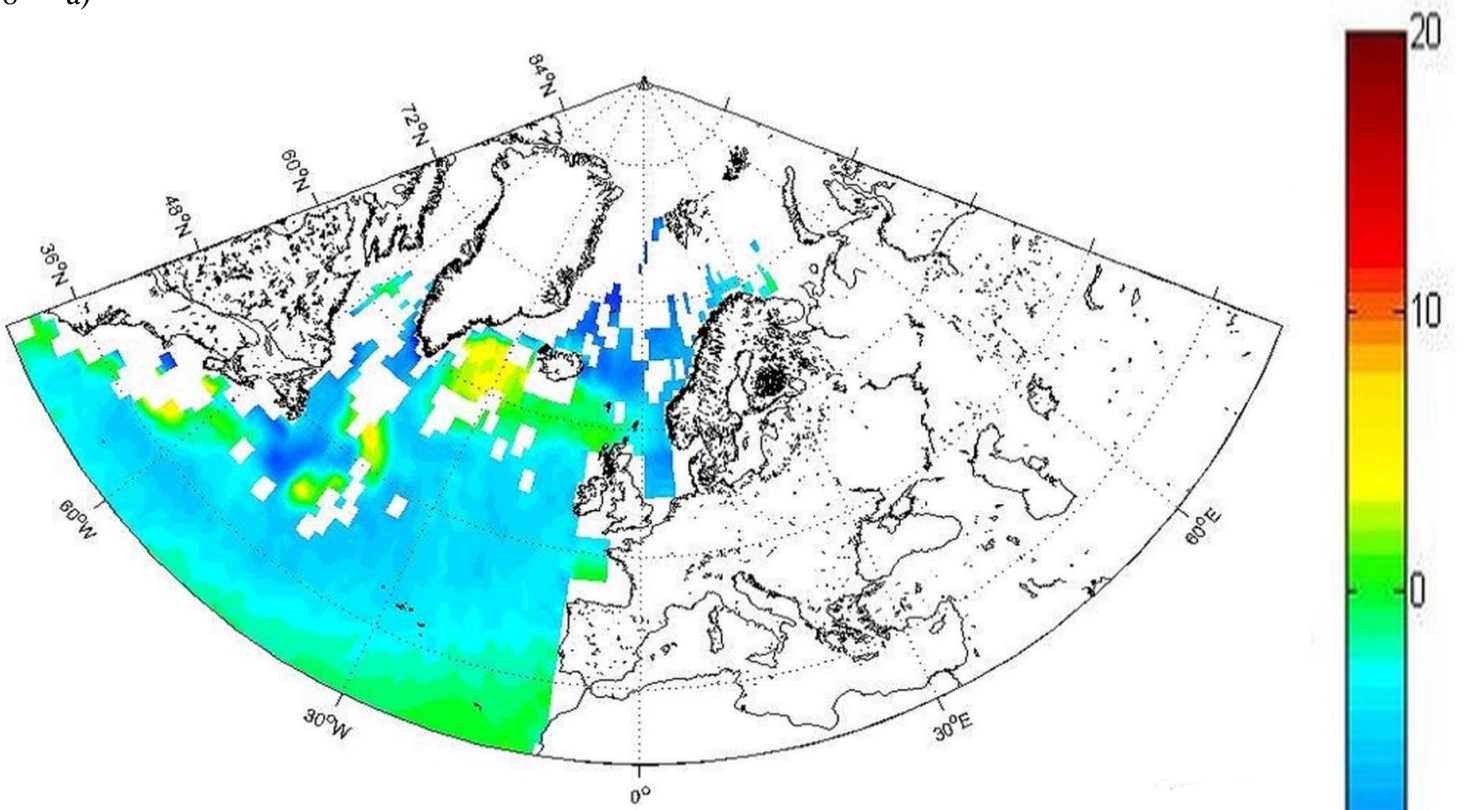
591 Figure 8. Comparison of monthly values fluxes of air-sea CO₂ fluxes calculated with different *p*CO₂
592 climatologies (Takahashi et al. 2009, SOCAT v. 1.5 and 2.0) using the same *k* parameterization
593 (Nightingale et al. 2000) in a) North Atlantic, b) European Arctic.

594

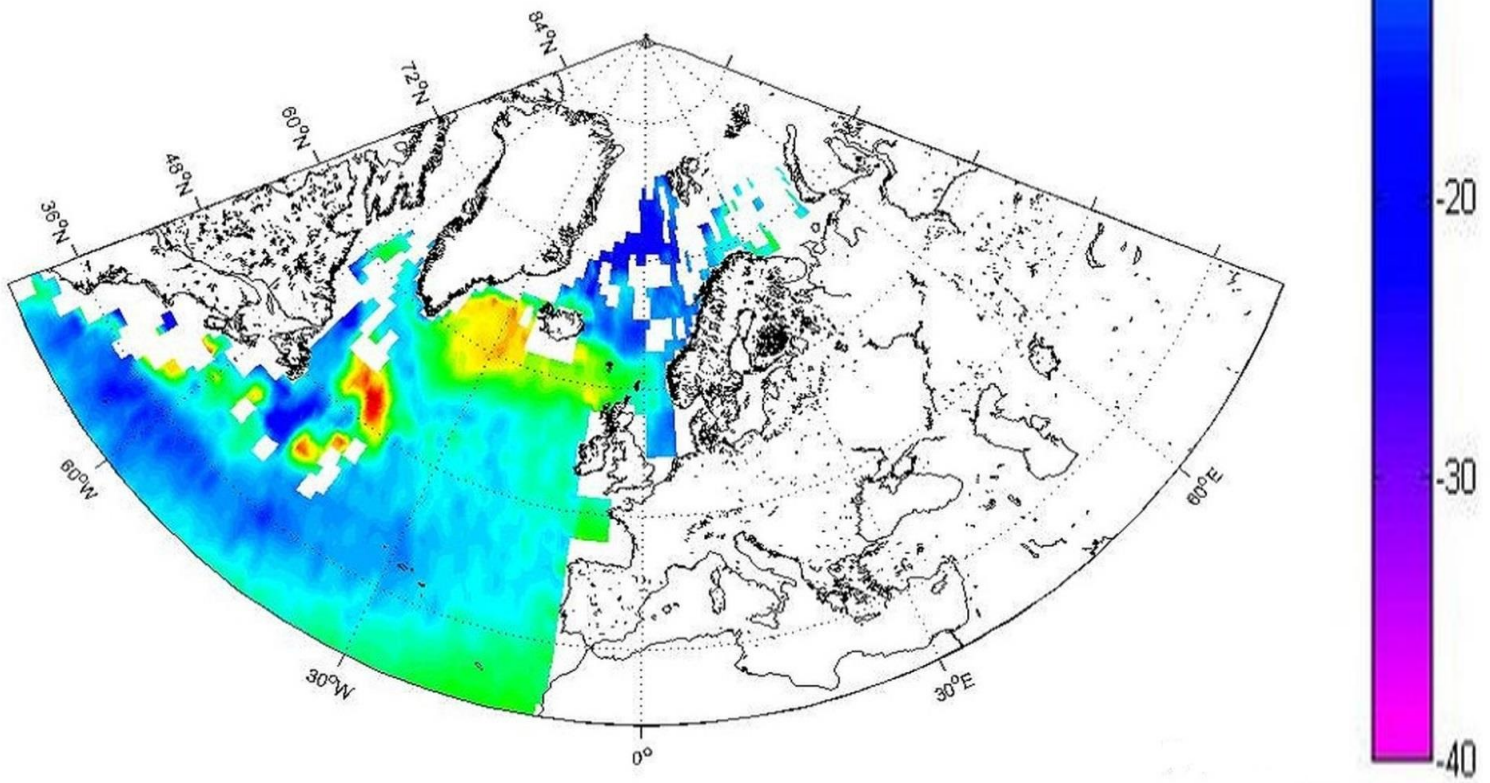
595 Figure 9. Different *k*660 parameterizations as a function of wind speed.

596

597
598 a)



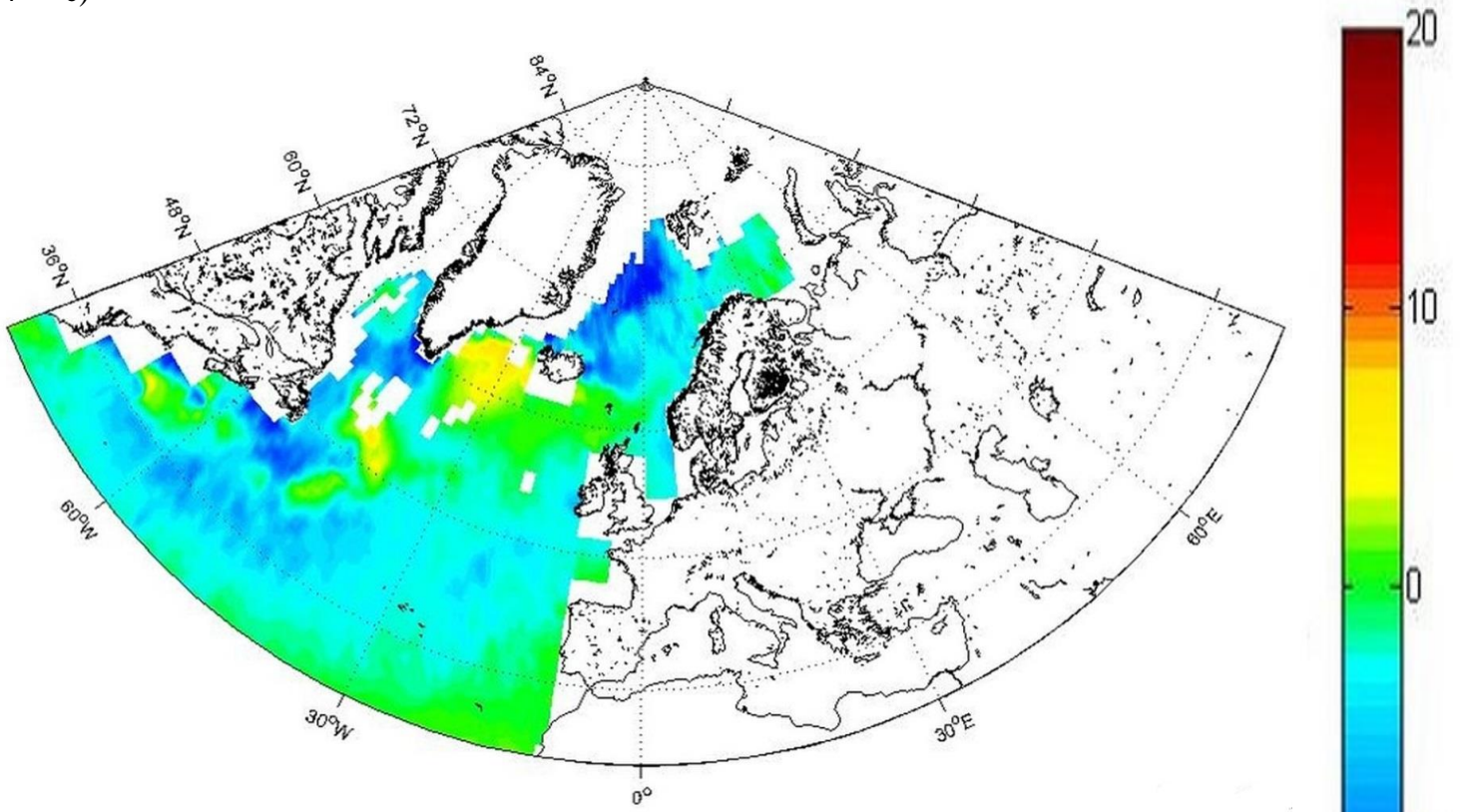
599
600 b)



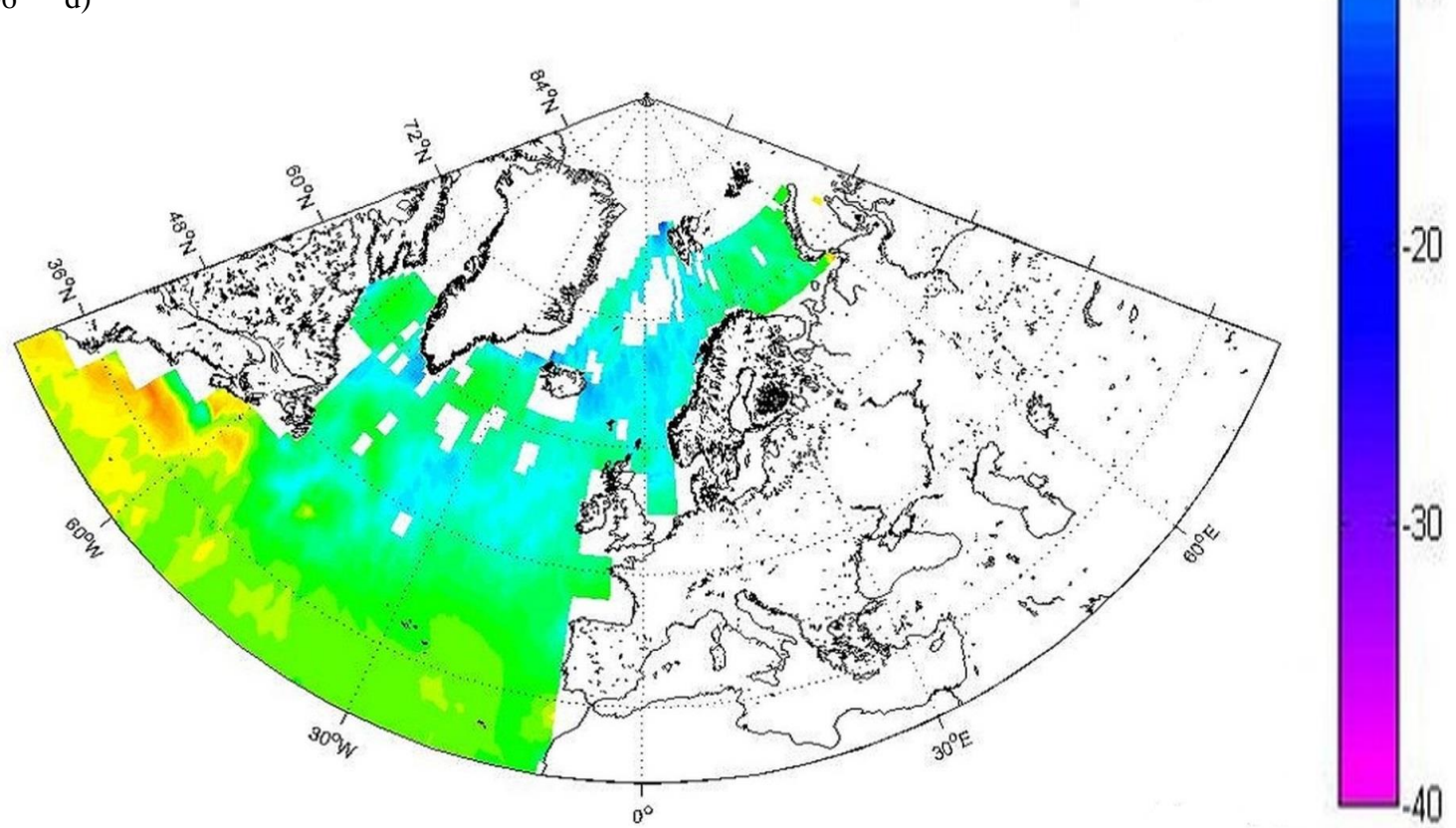
601
602
13

(mg C m⁻² day⁻¹)

603
604 c)



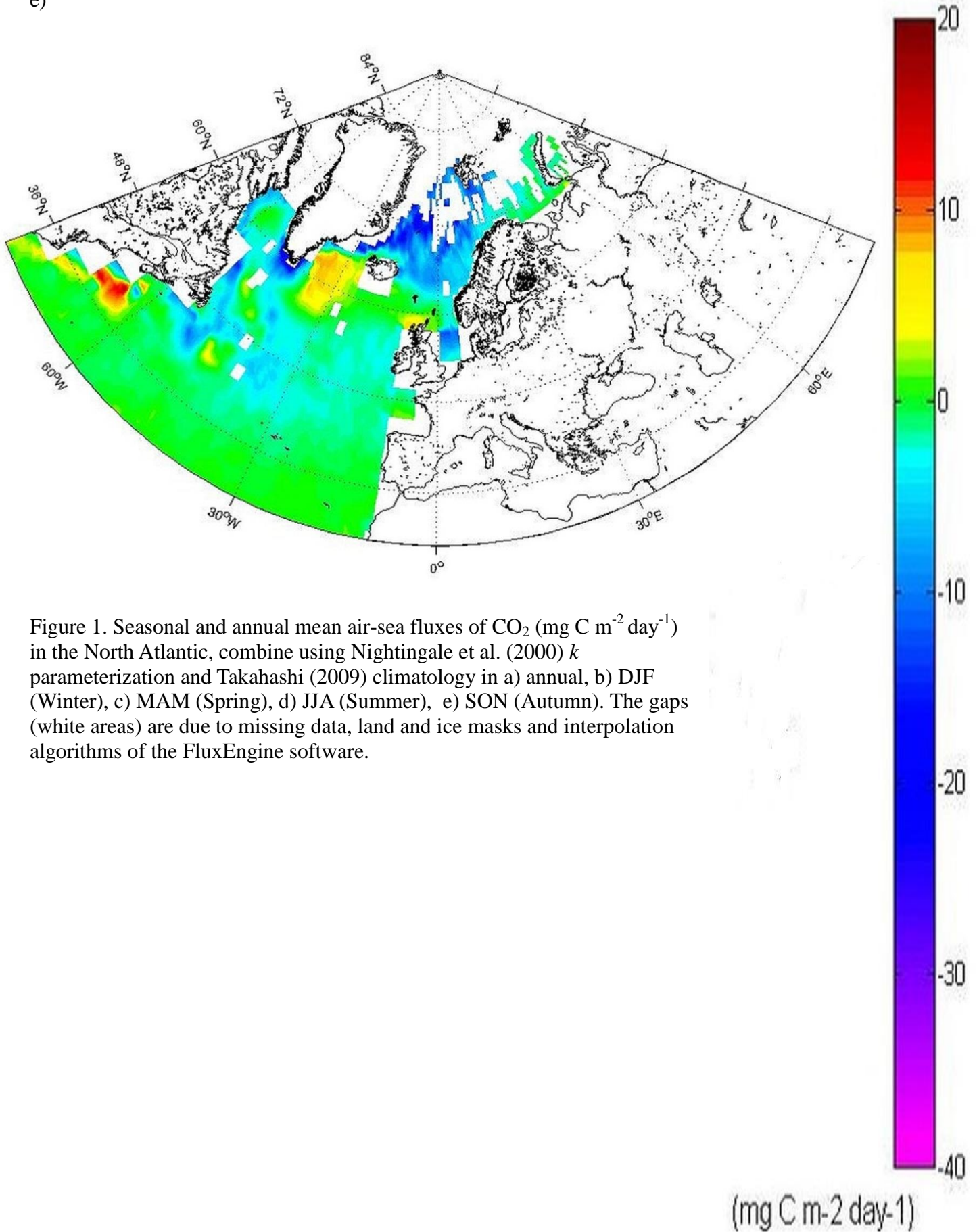
605
606 d)



607
608

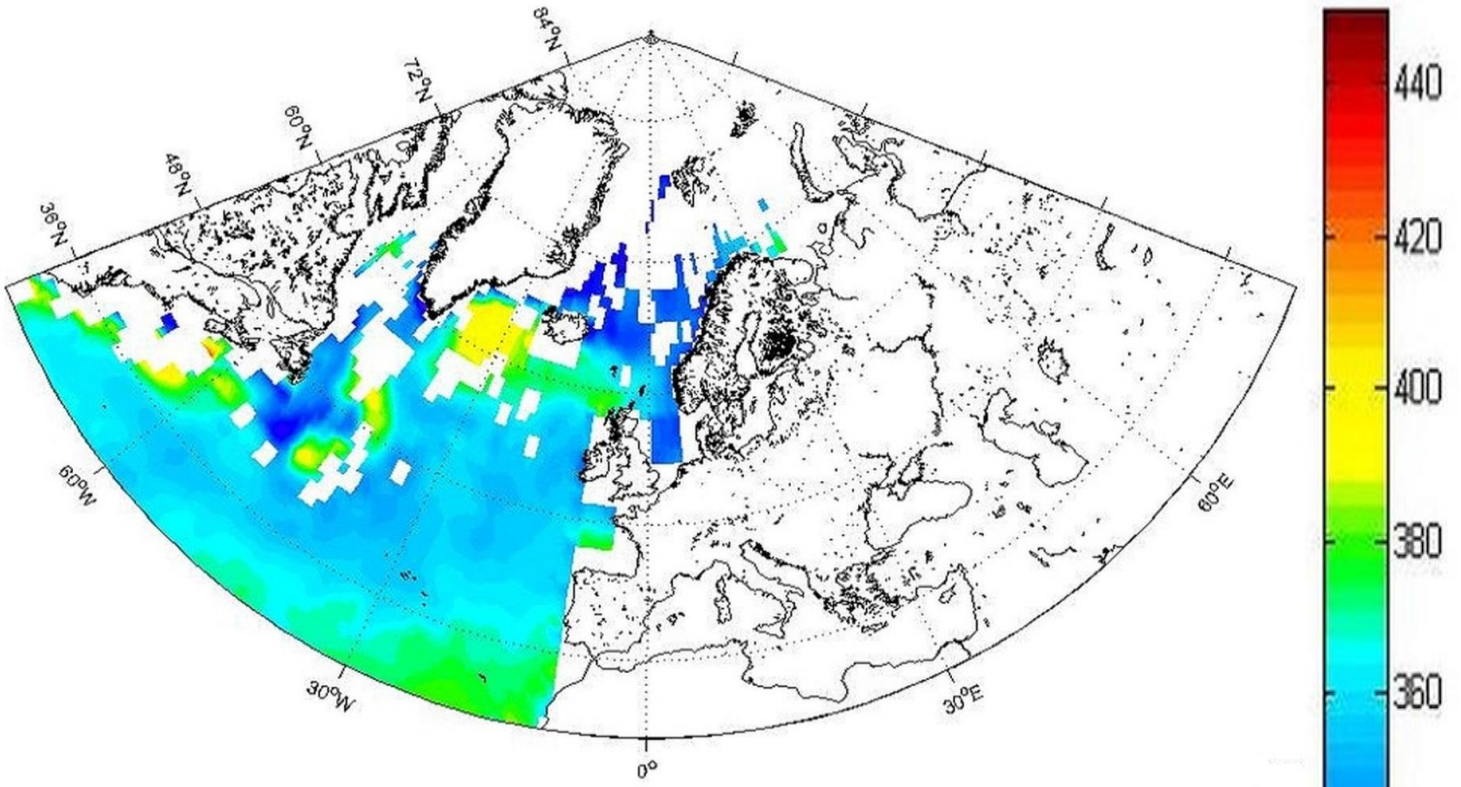
(mg C m⁻² day⁻¹)

609
610 e)

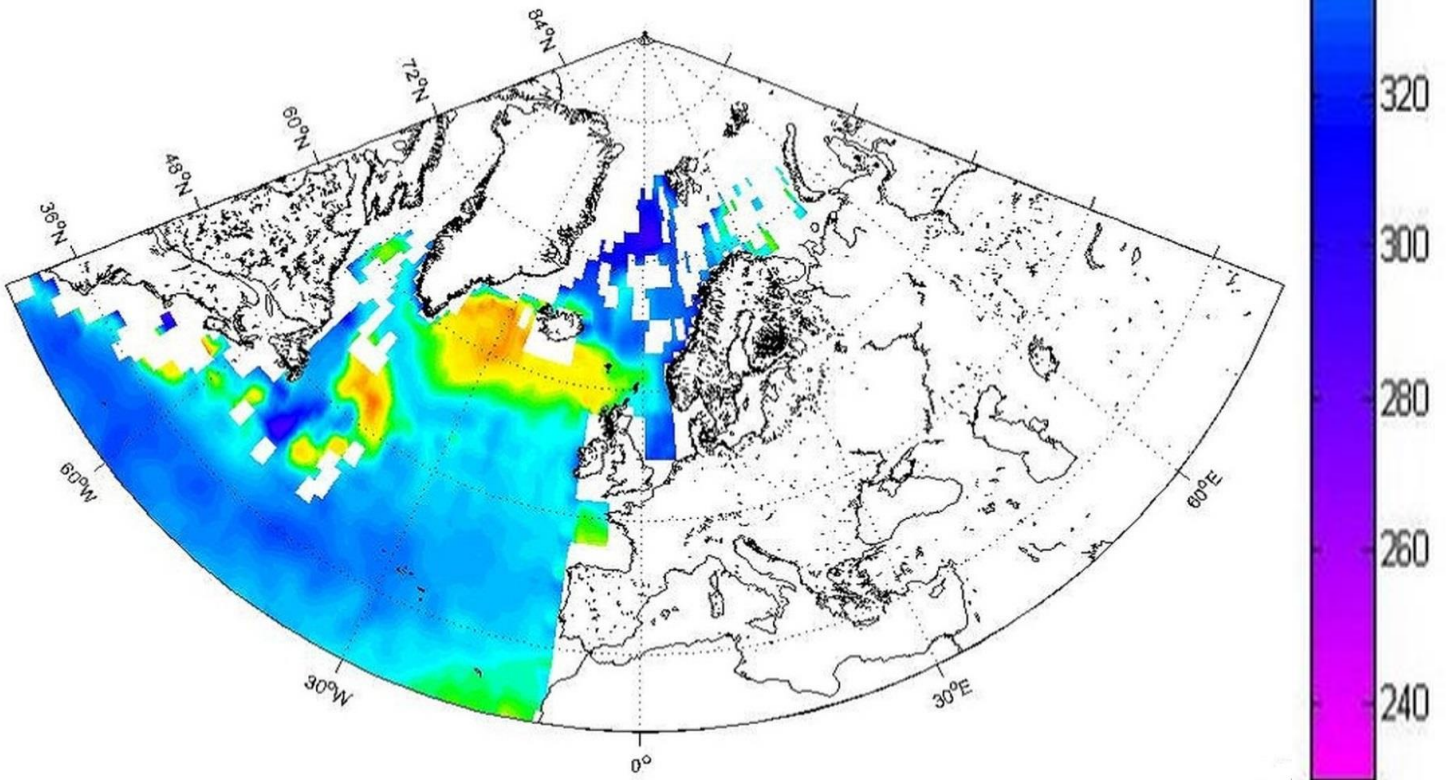


611
612 Figure 1. Seasonal and annual mean air-sea fluxes of CO₂ (mg C m⁻² day⁻¹)
613 in the North Atlantic, combine using Nightingale et al. (2000) *k*
614 parameterization and Takahashi (2009) climatology in a) annual, b) DJF
615 (Winter), c) MAM (Spring), d) JJA (Summer), e) SON (Autumn). The gaps
616 (white areas) are due to missing data, land and ice masks and interpolation
617 algorithms of the FluxEngine software.

618
619 a)



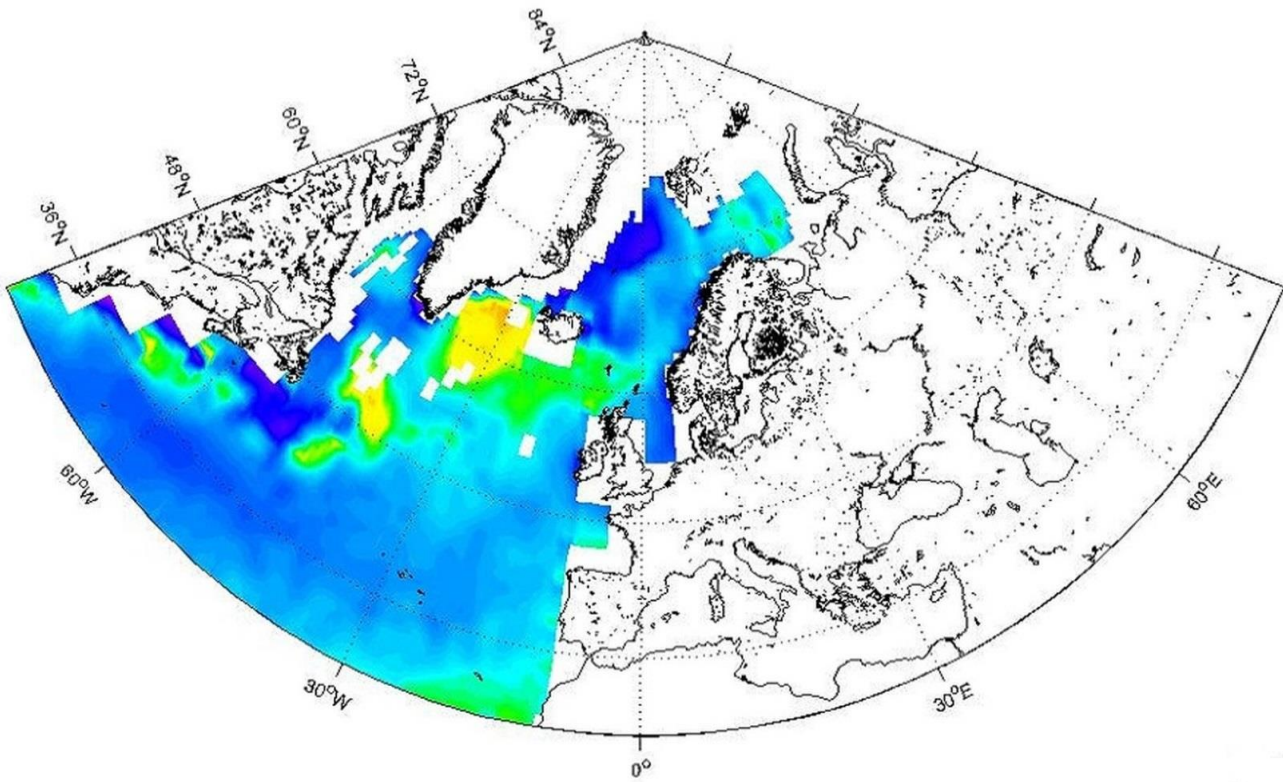
620
621 b)



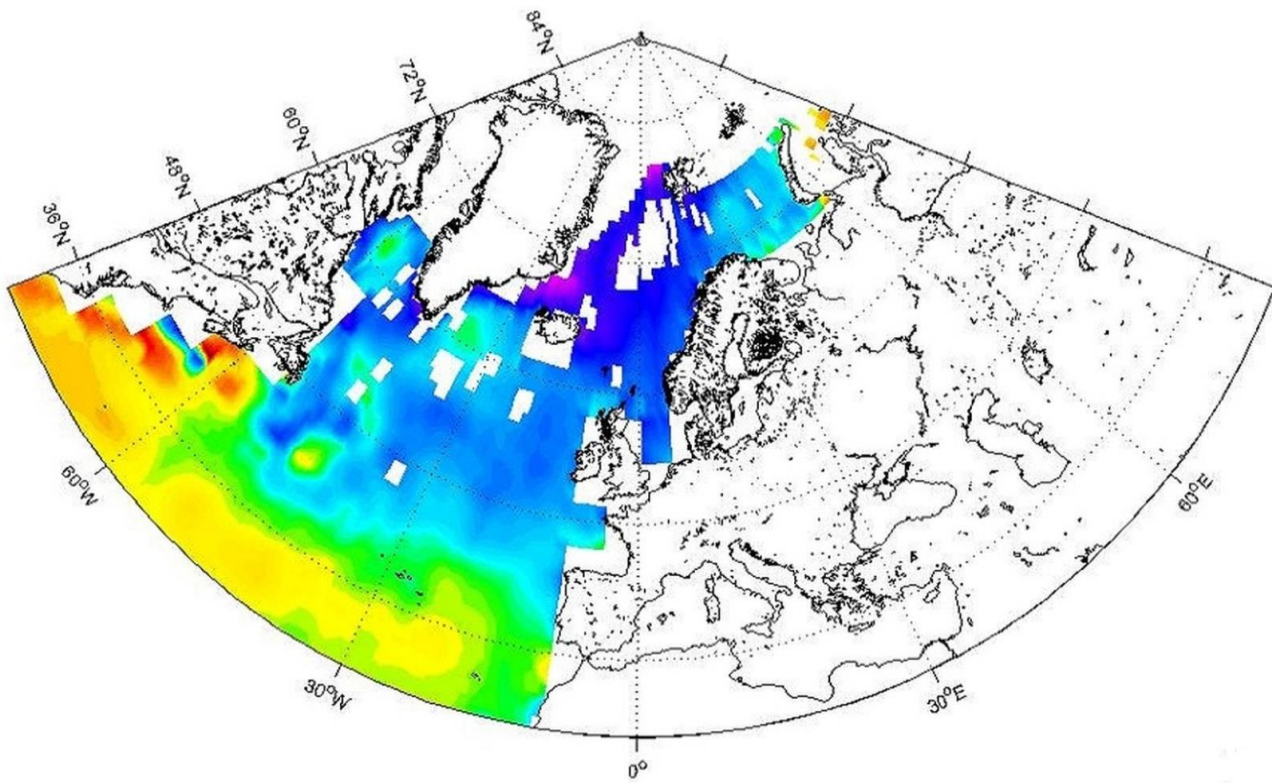
622
623

(microatm)

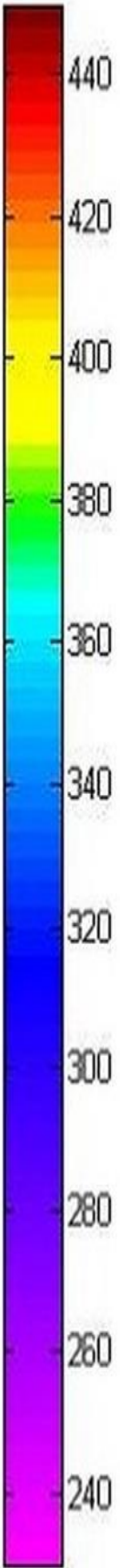
624
625 c)



626
627 d)

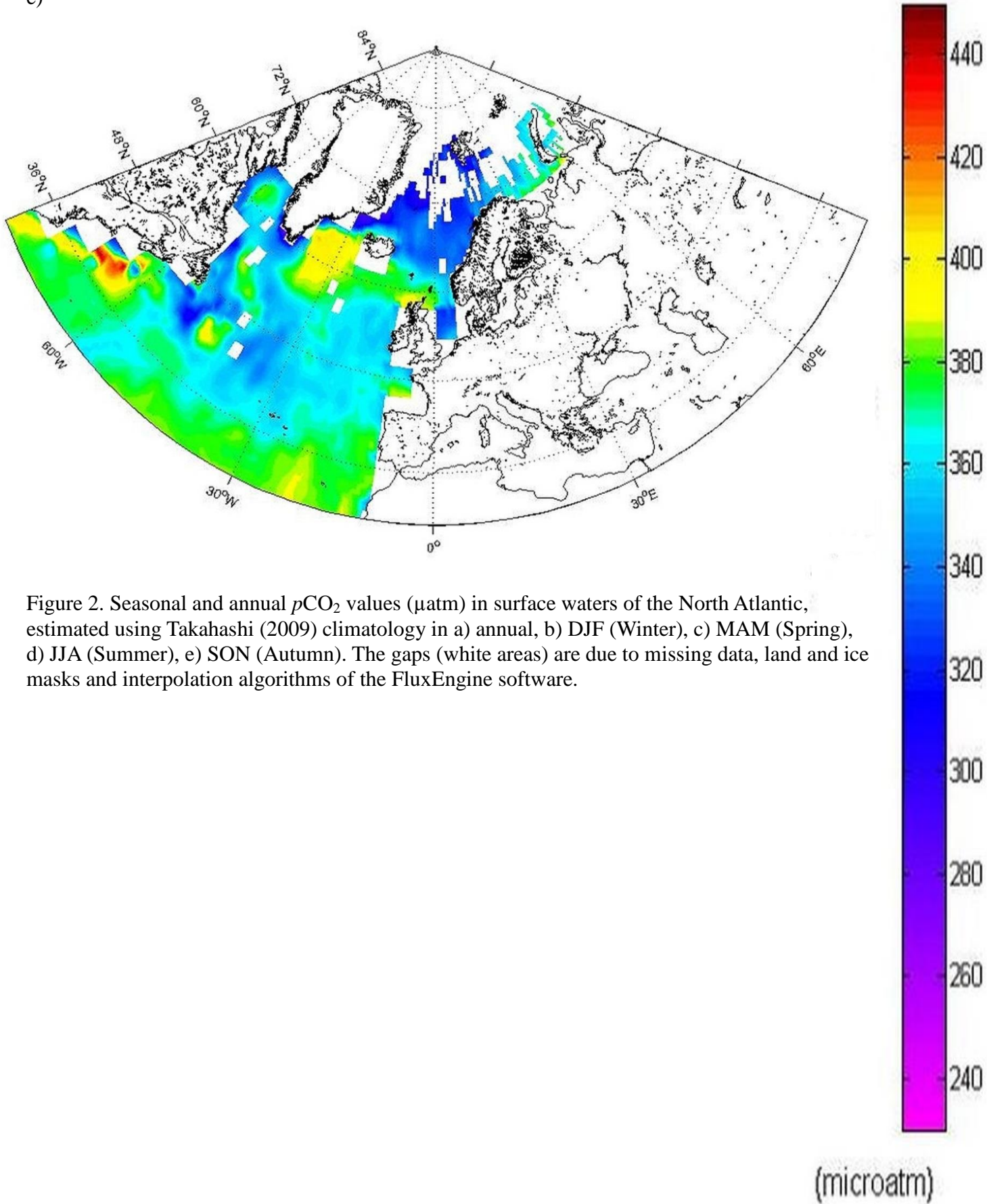


628
629



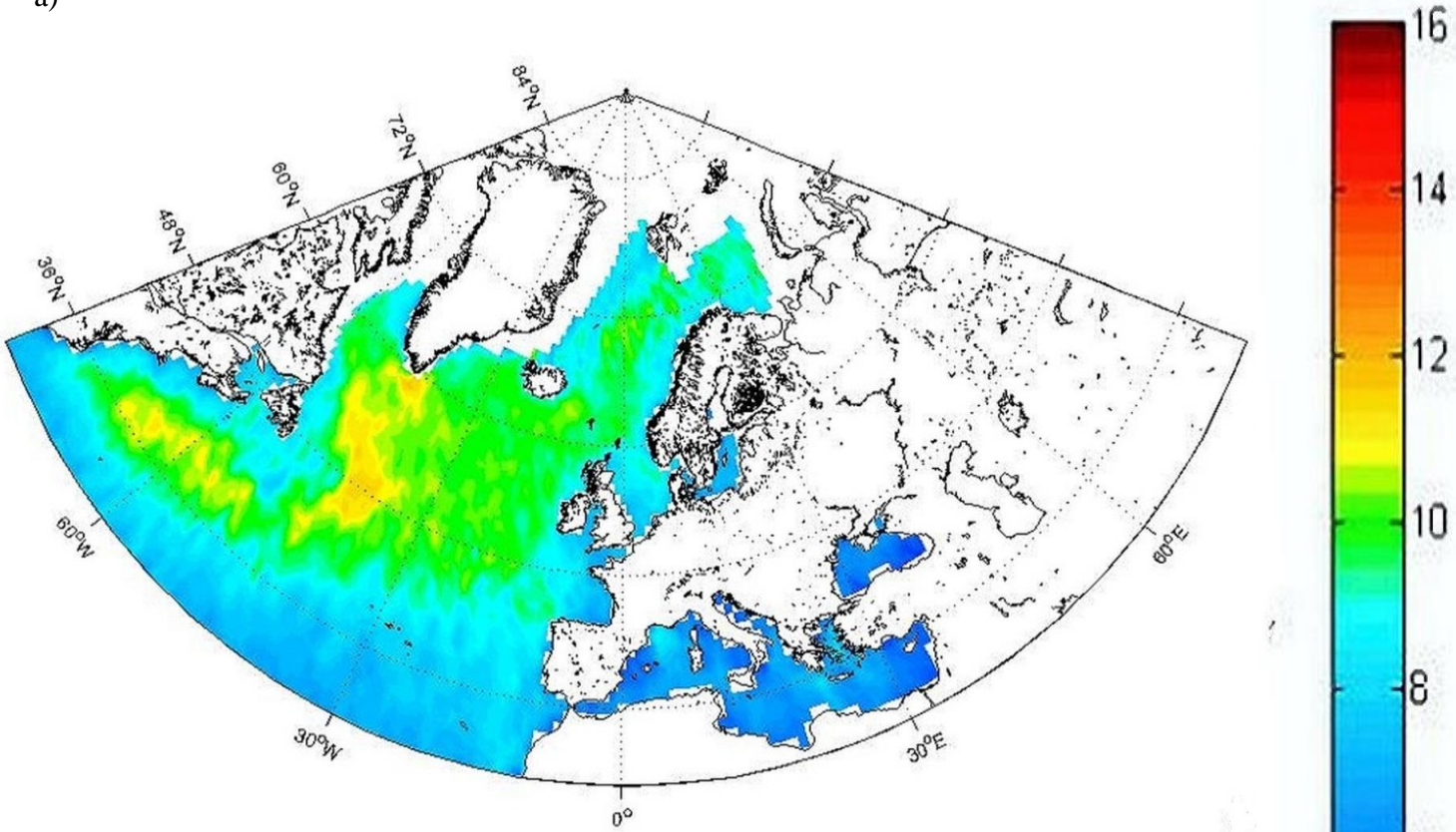
(microatm)

630
631 e)

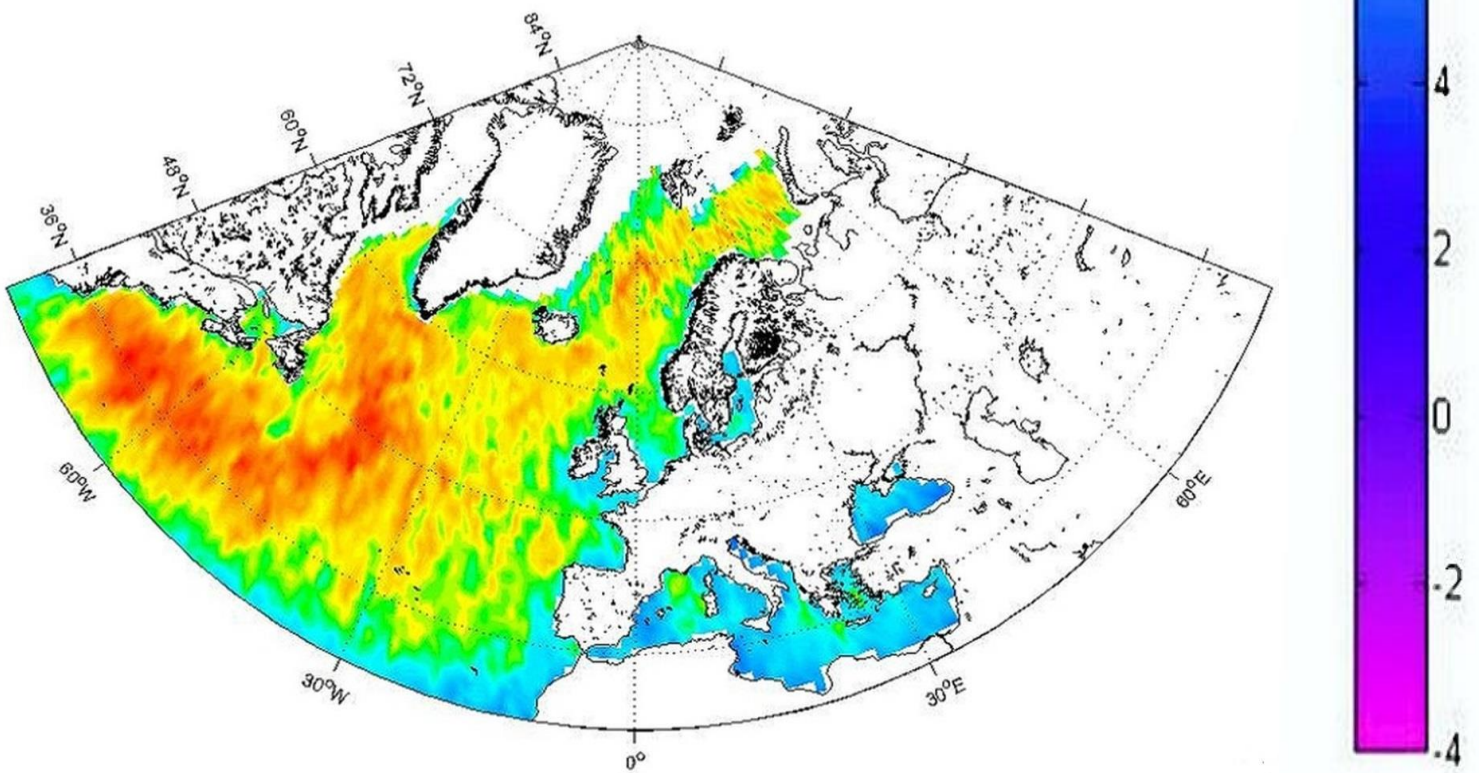


632
633
634
635
636
637
638

639
640 a)



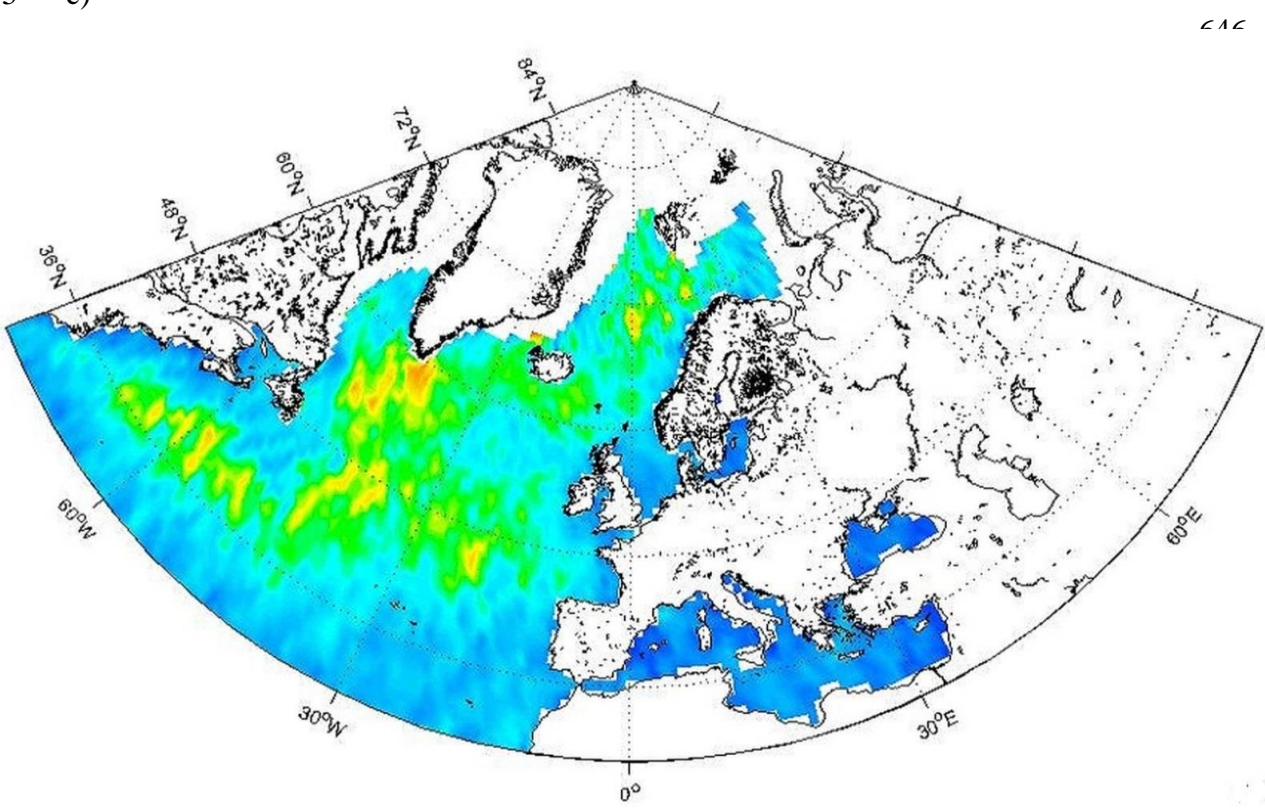
641 b)



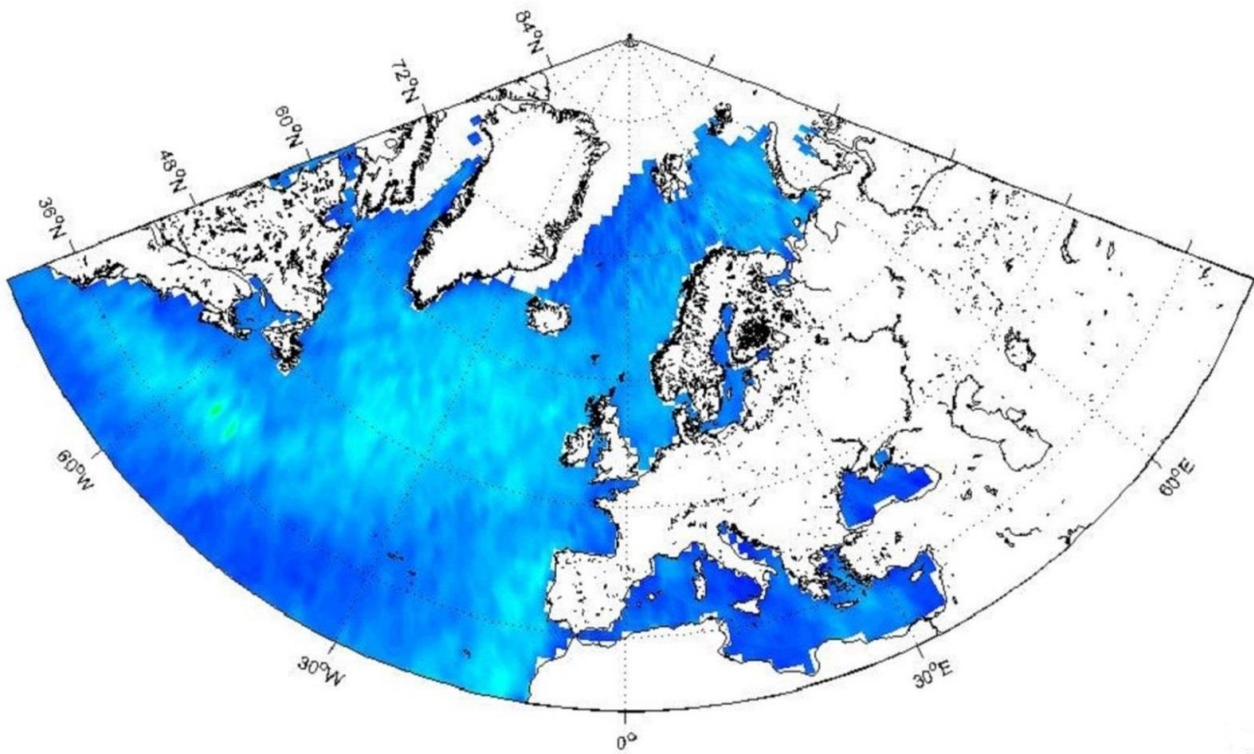
642
643

(m s⁻¹)

644
645 c)



669
670 d)



646

671

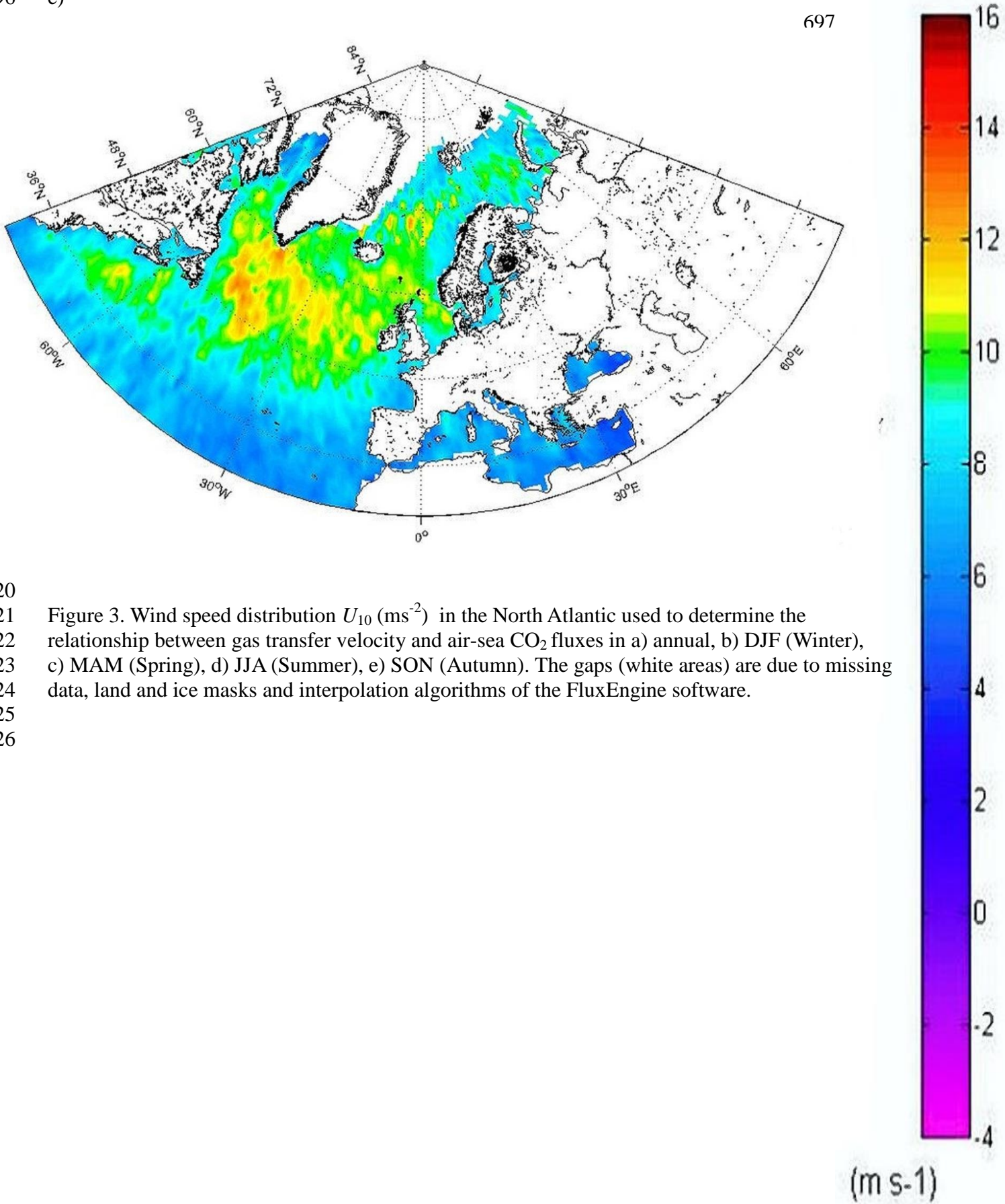


(m s⁻¹)

694

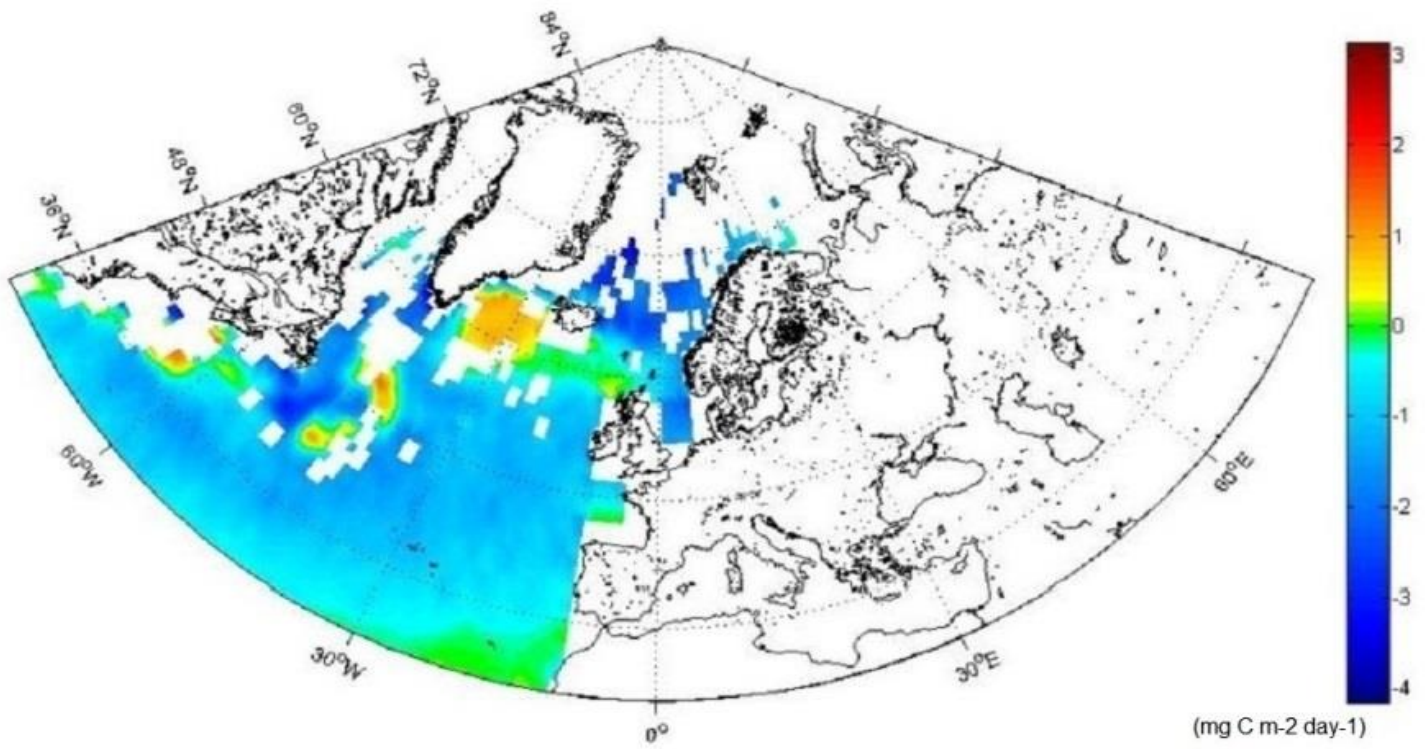
695
696 e)

697

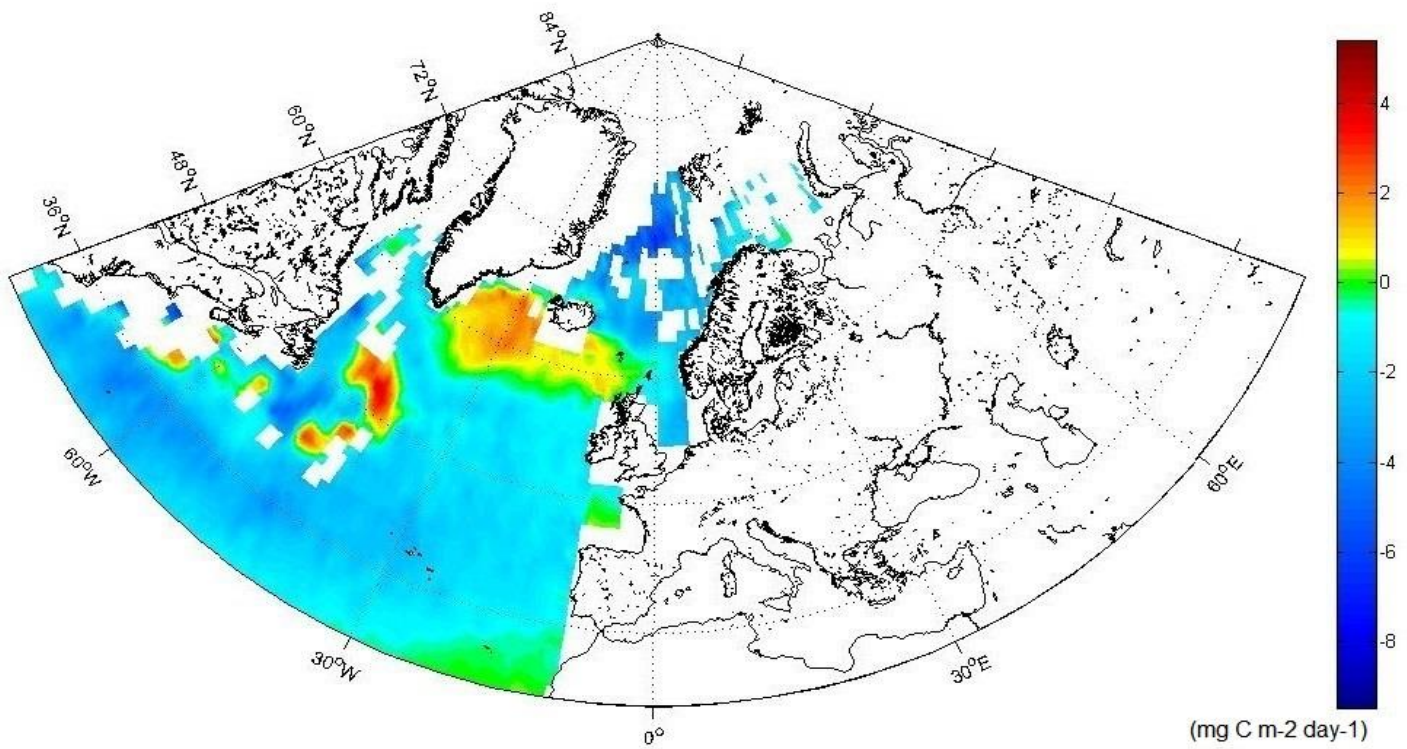


720
721 Figure 3. Wind speed distribution U_{10} (ms^{-2}) in the North Atlantic used to determine the
722 relationship between gas transfer velocity and air-sea CO_2 fluxes in a) annual, b) DJF (Winter),
723 c) MAM (Spring), d) JJA (Summer), e) SON (Autumn). The gaps (white areas) are due to missing
724 data, land and ice masks and interpolation algorithms of the FluxEngine software.
725
726

727
728 a)

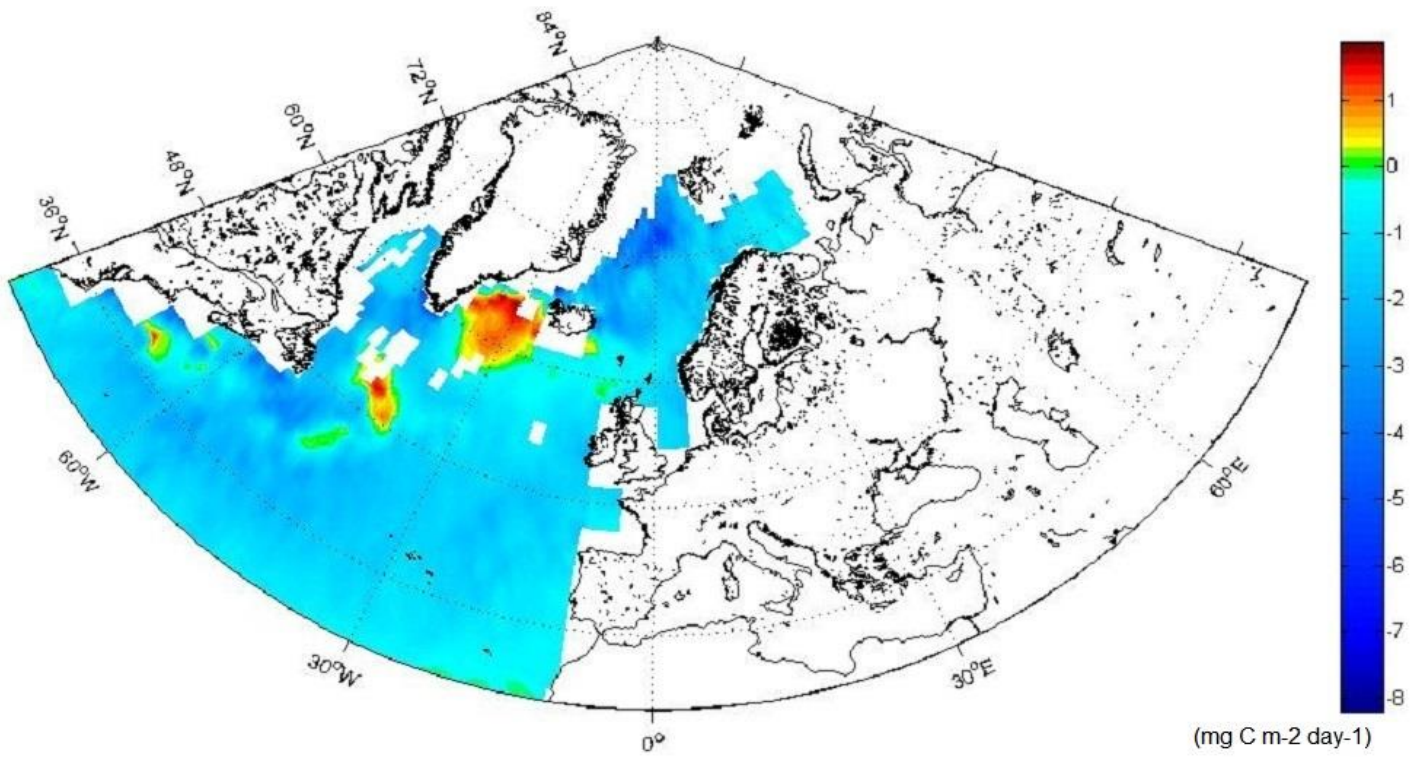


729
730 b)

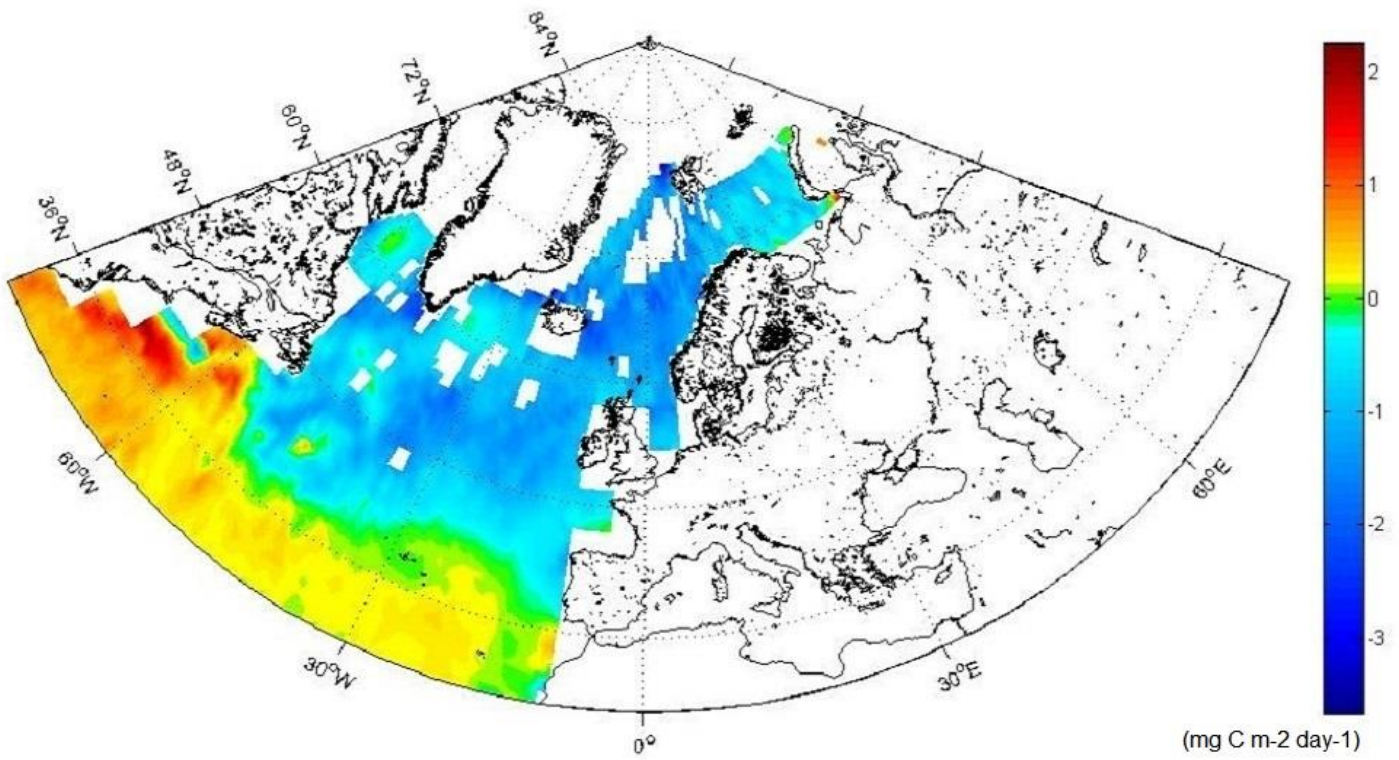


731
732

733
734 c)

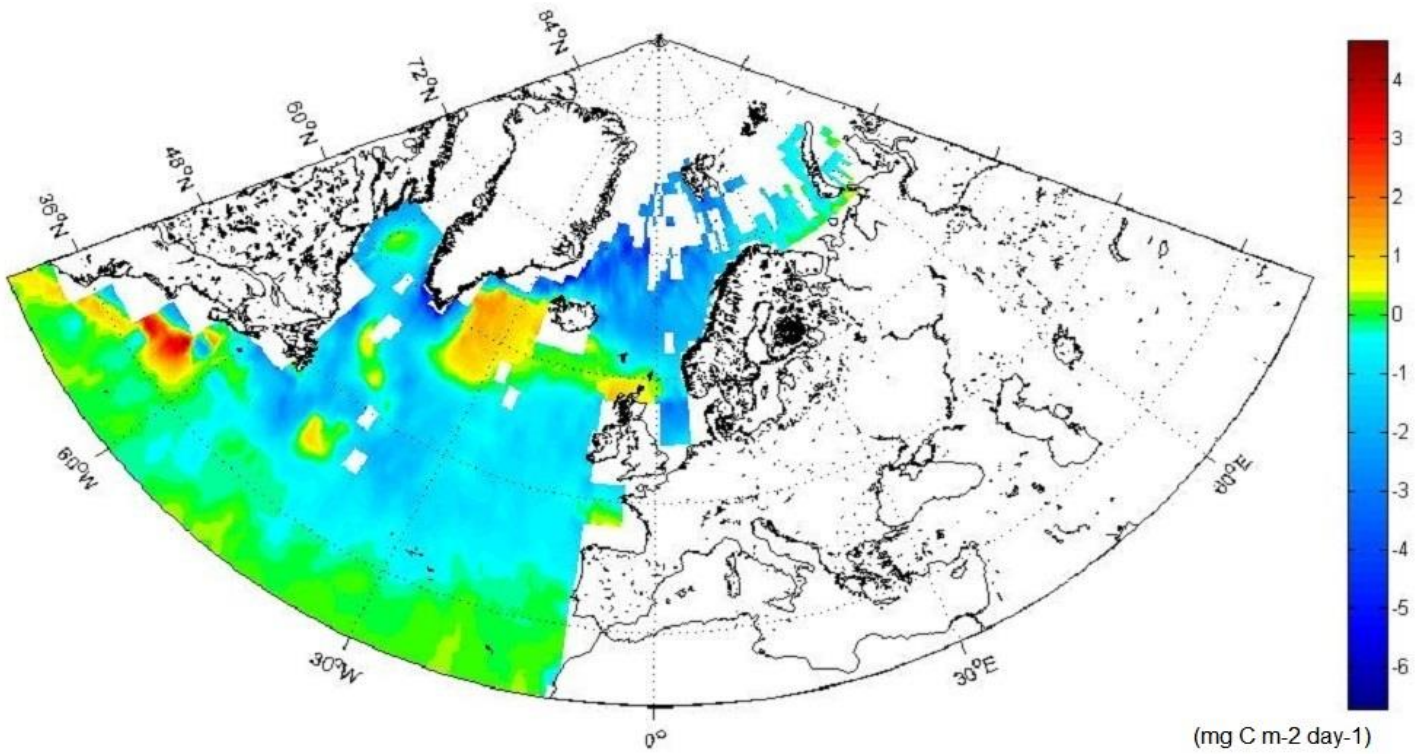


735
736 d)



737
738

739
740 e)

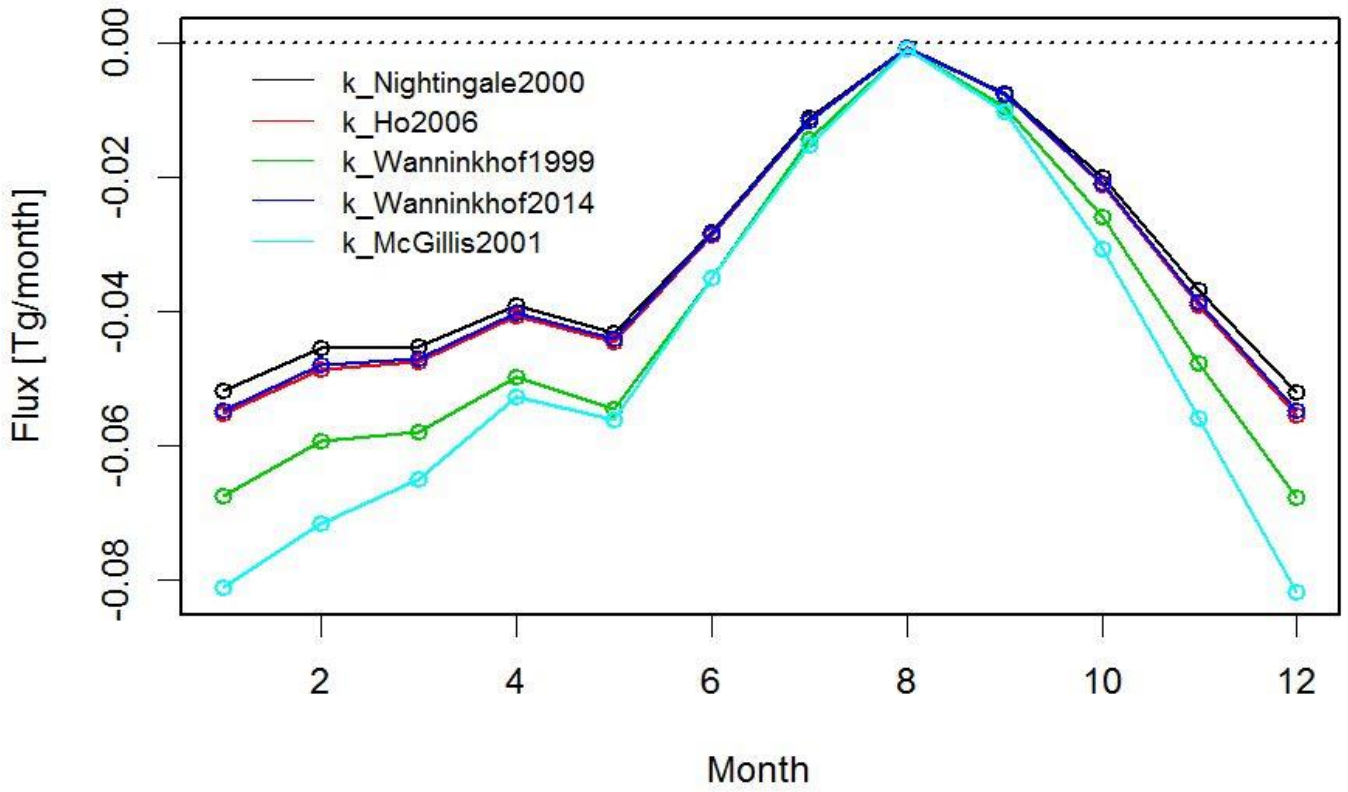


741
742 Figure 4. Differences maps for the air-sea CO₂ fluxes (mg C m⁻² day⁻¹) in the North Atlantic,
743 between a wind cubed and squared parameterizations (Wanninkhof and McGillis 1999 and
744 Wanninkhof 2014) in a) annual, b) DJF (Winter), c) MAM (Spring), d) JJA (Summer), e) SON
745 (Autumn). The gaps (white areas) are due to missing data, land and ice masks and interpolation
746 algorithms of the FluxEngine software.

747

748

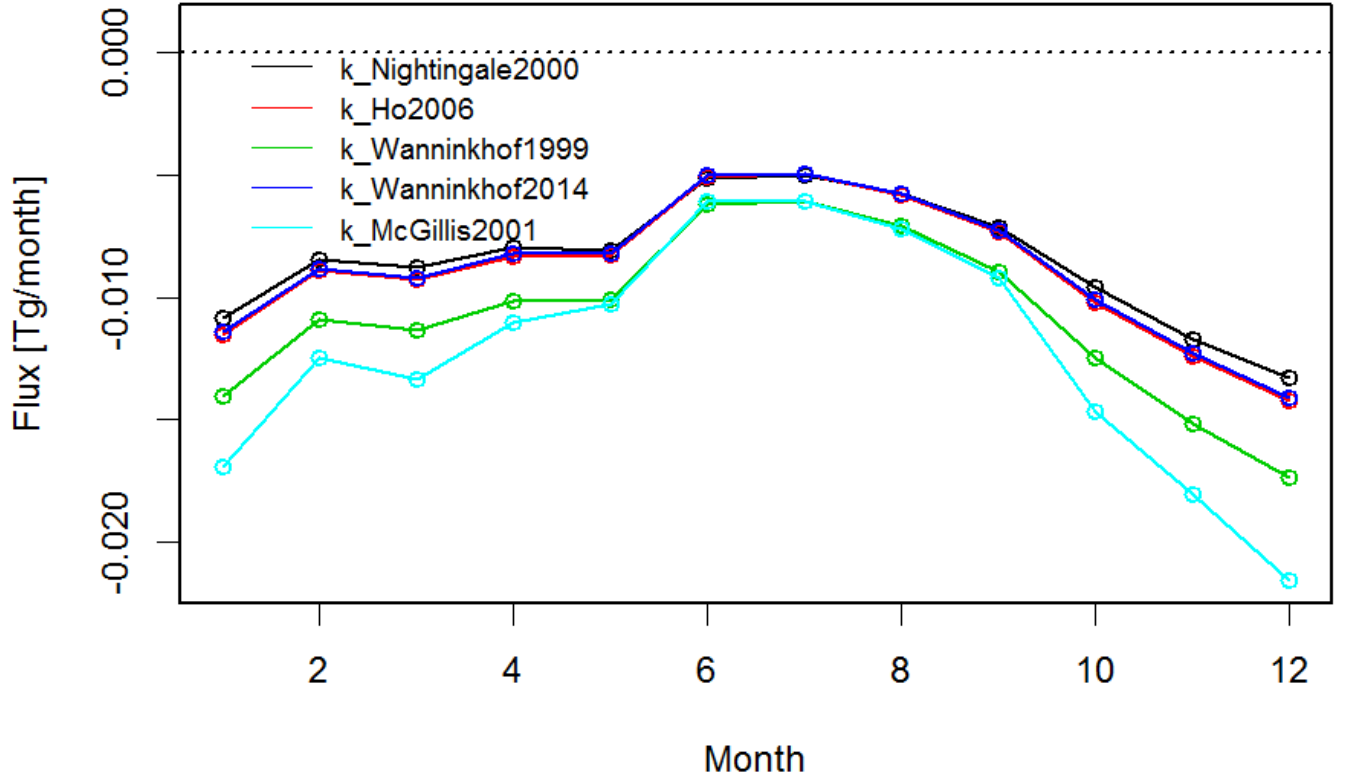
a)



749

750

b)



751

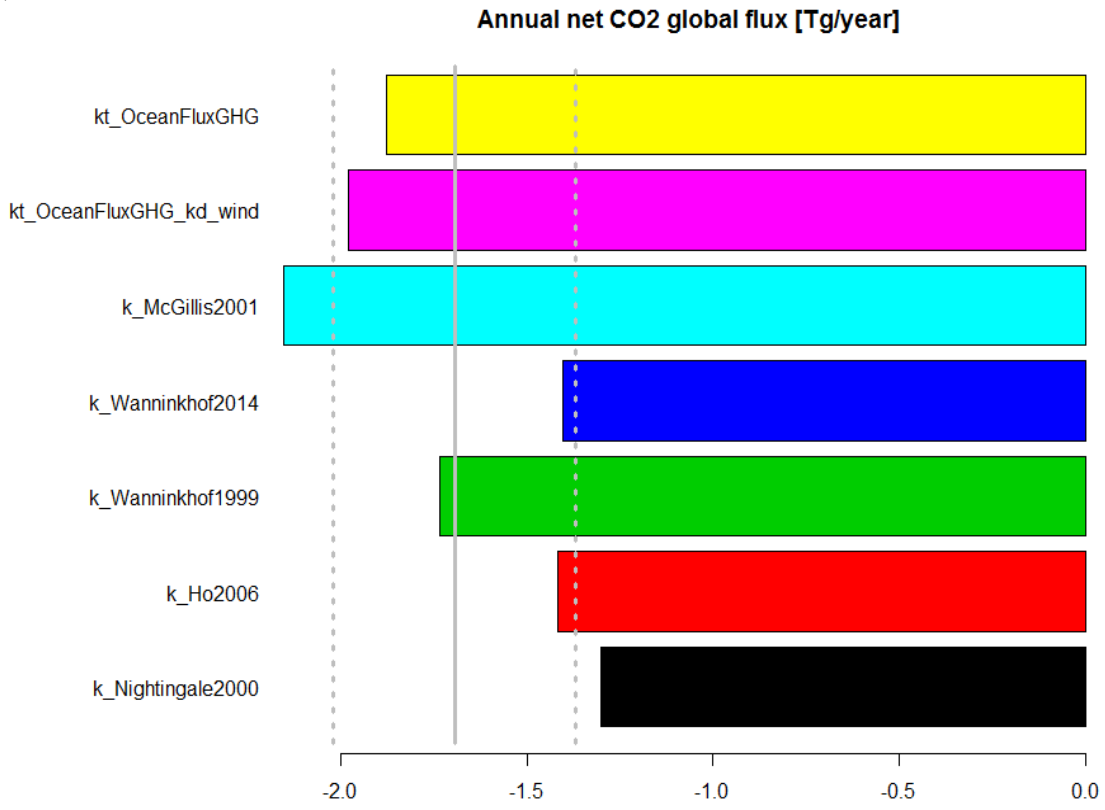
752

753

Figure 5. Monthly values air-sea fluxes of CO₂ (Tg/month) for the five parameterizations (eq. 4-8) in a) North Atlantic, b) European Arctic.

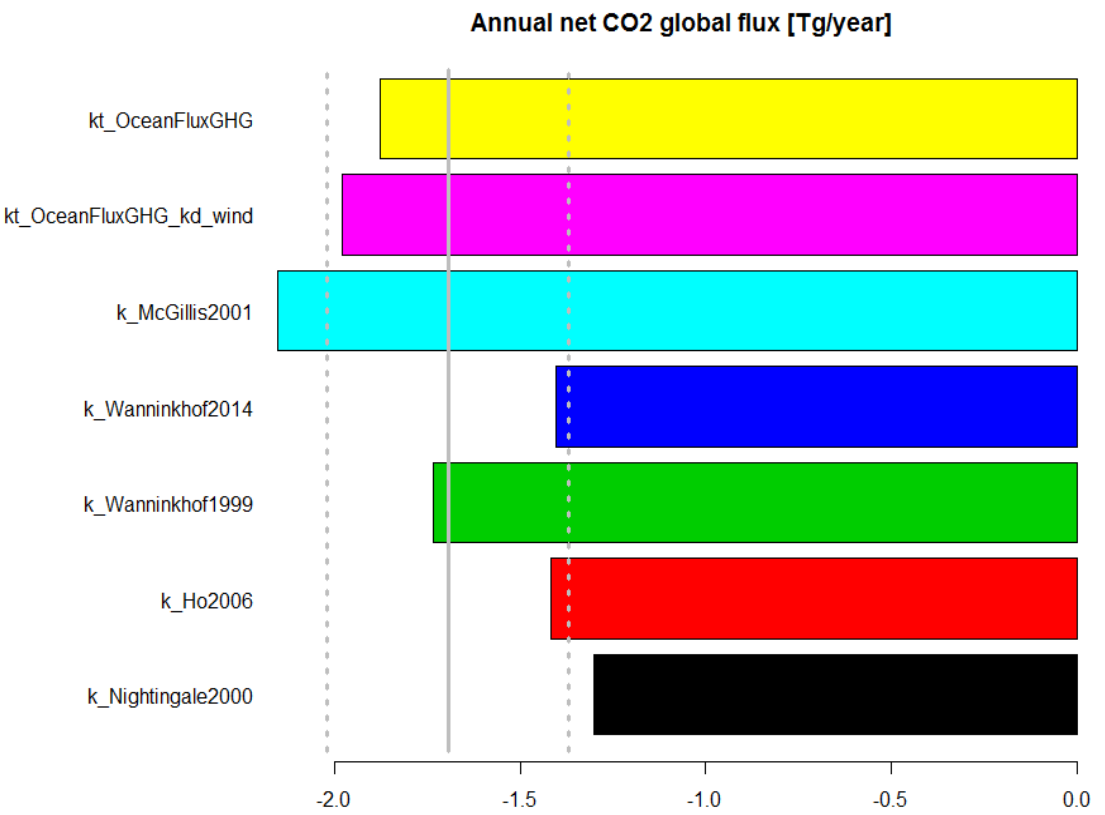
754
755

a)



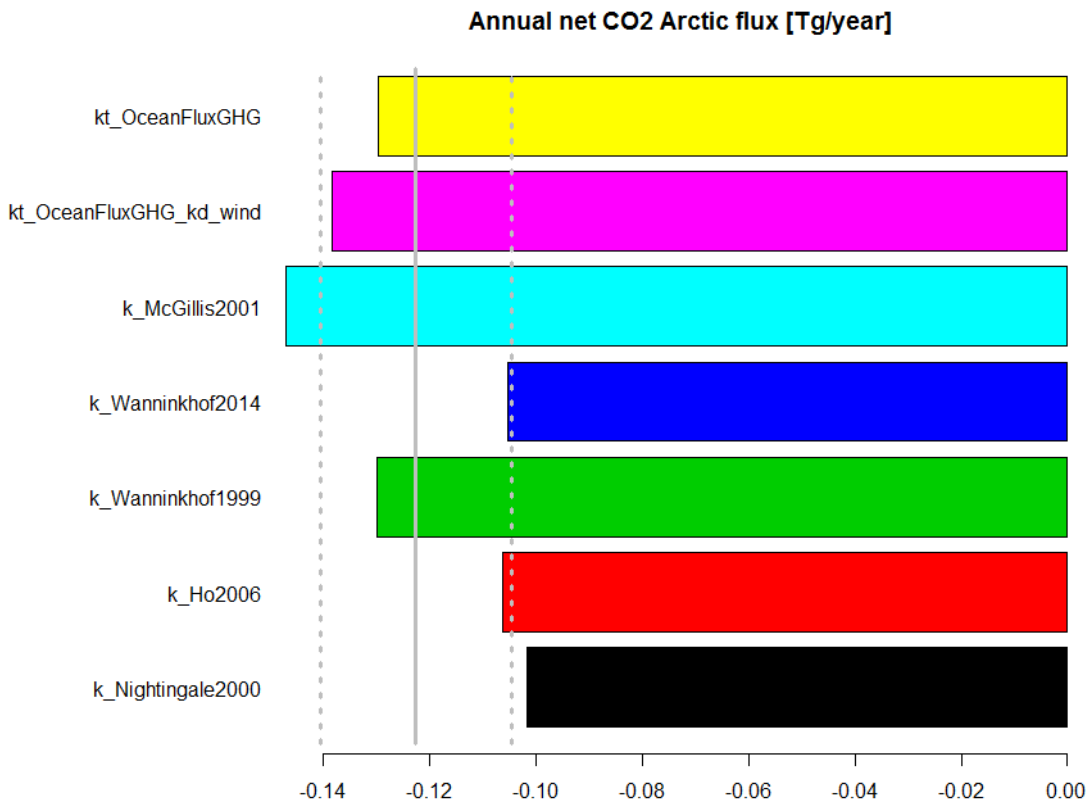
756
757

b)



758
759
760
761
762

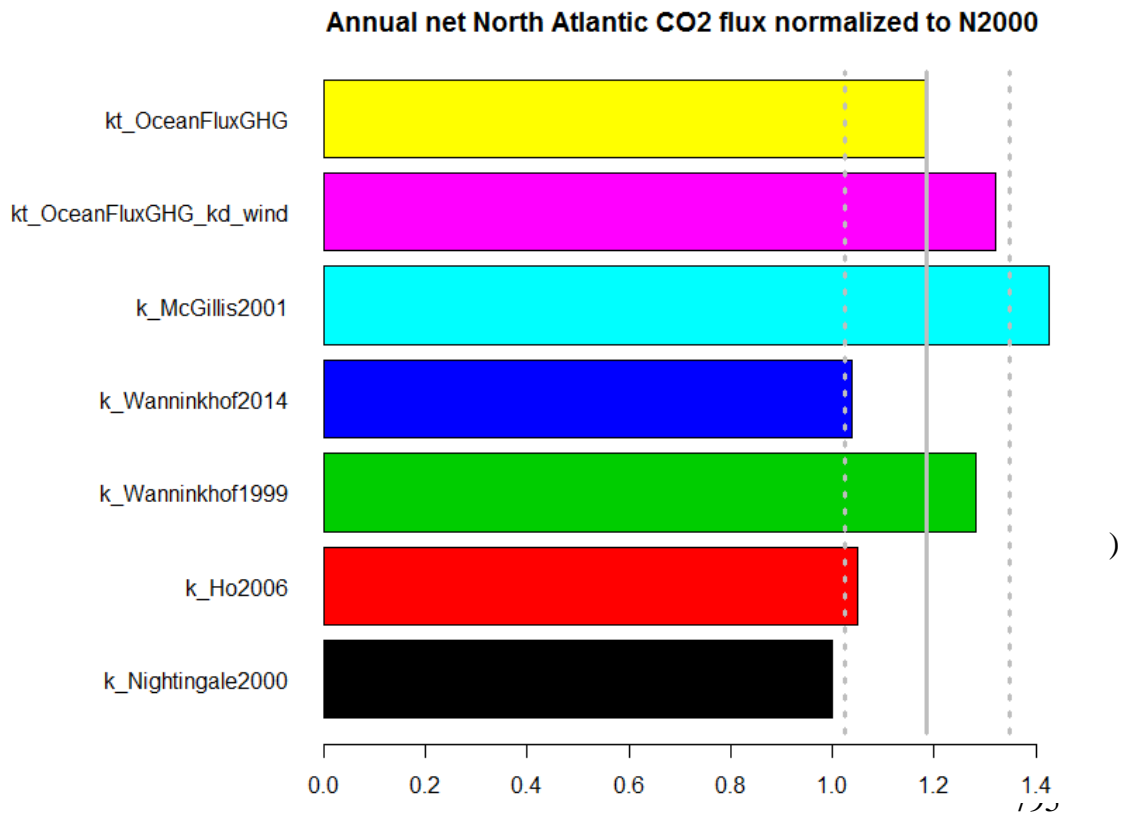
763
764 c)



765
766 Figure 6. Annual air-sea fluxes of CO₂ (Tg/year) for the five (eq. 4-8) parameterizations as well as
767 for backscatter (default) and wind driven OceanFluxGHG parameterization (see text) in a) global, b)
768 North Atlantic, c) European Arctic. Average values for all parameterization and standard deviations
769 are marked as vertical gray lines.
770

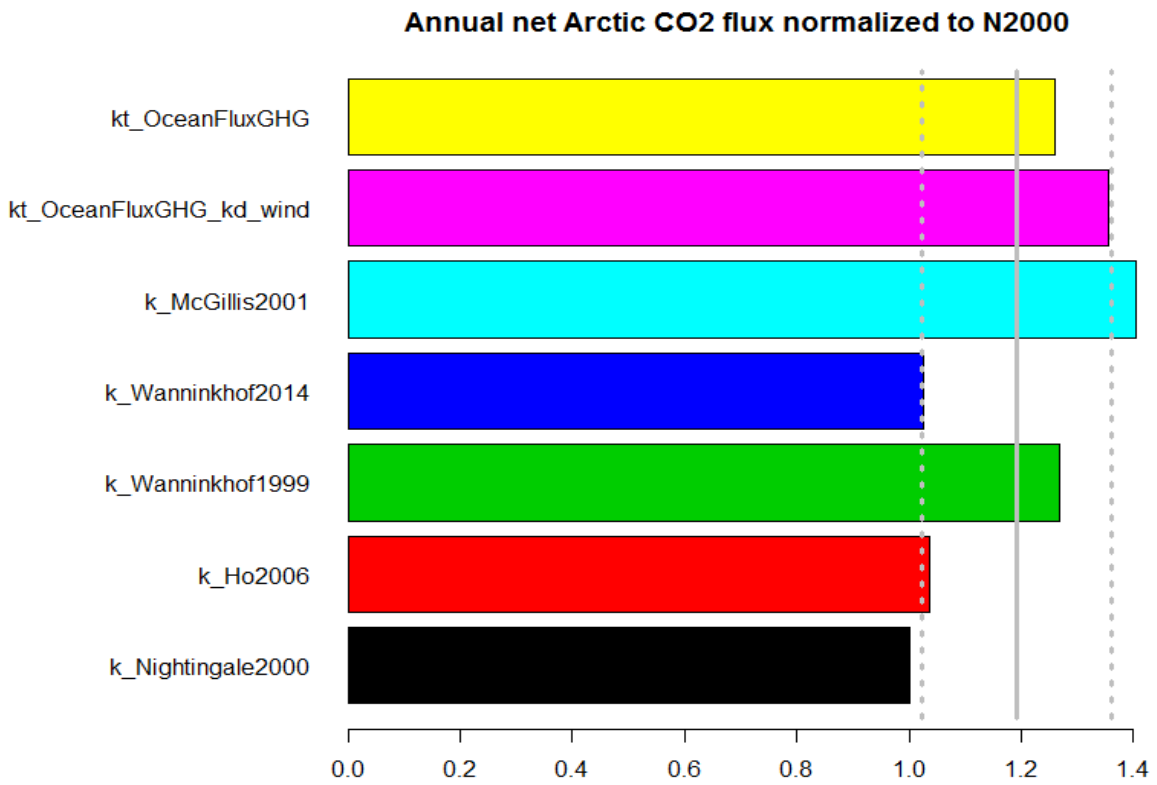
771

772 a)



796

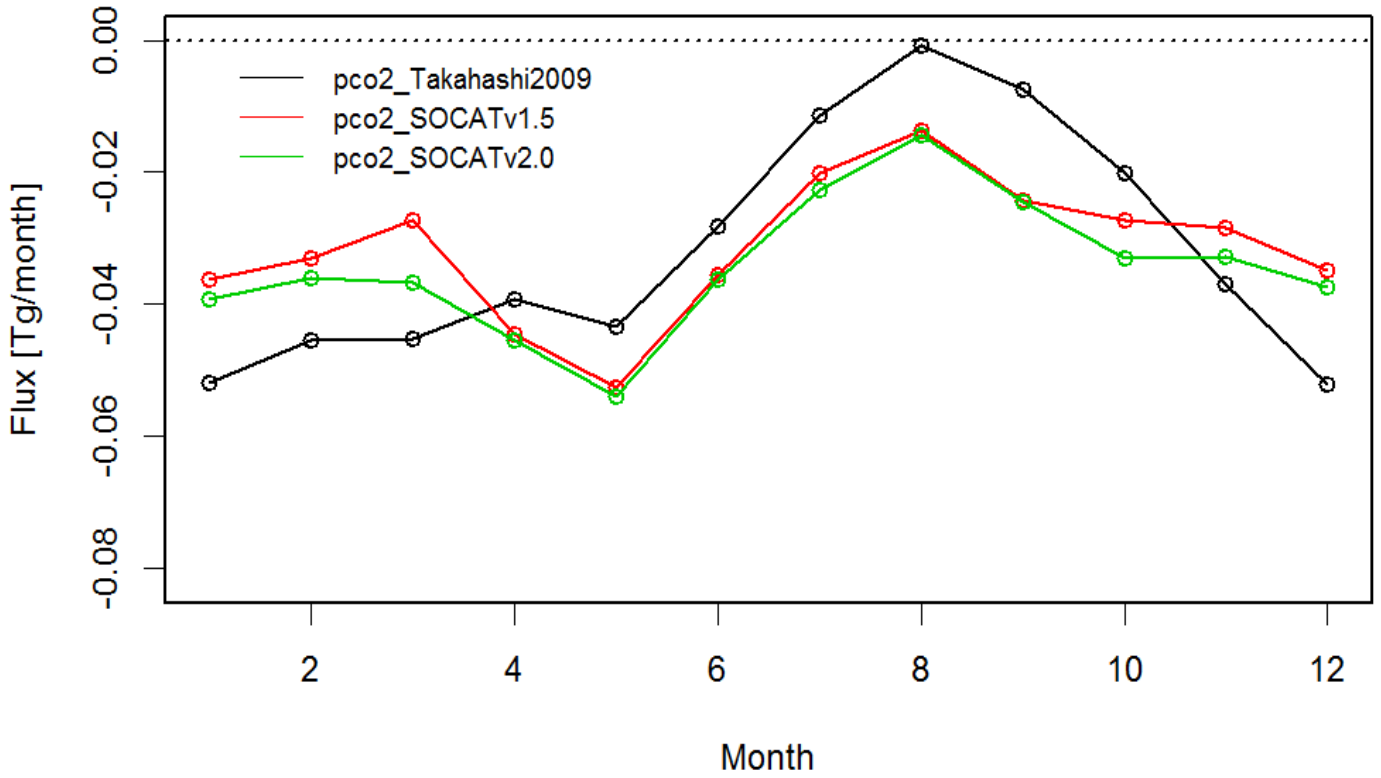
797 b)



798 Figure 7. Annual air-sea fluxes of CO₂ (Tg/year) for the five (eq. 4-8) parameterizations as well as
799 for backscatter (default) and wind driven OceanFluxGHG parameterization normalized to flux
800 values of Nightingale et al. (2000) *k* parameterization.

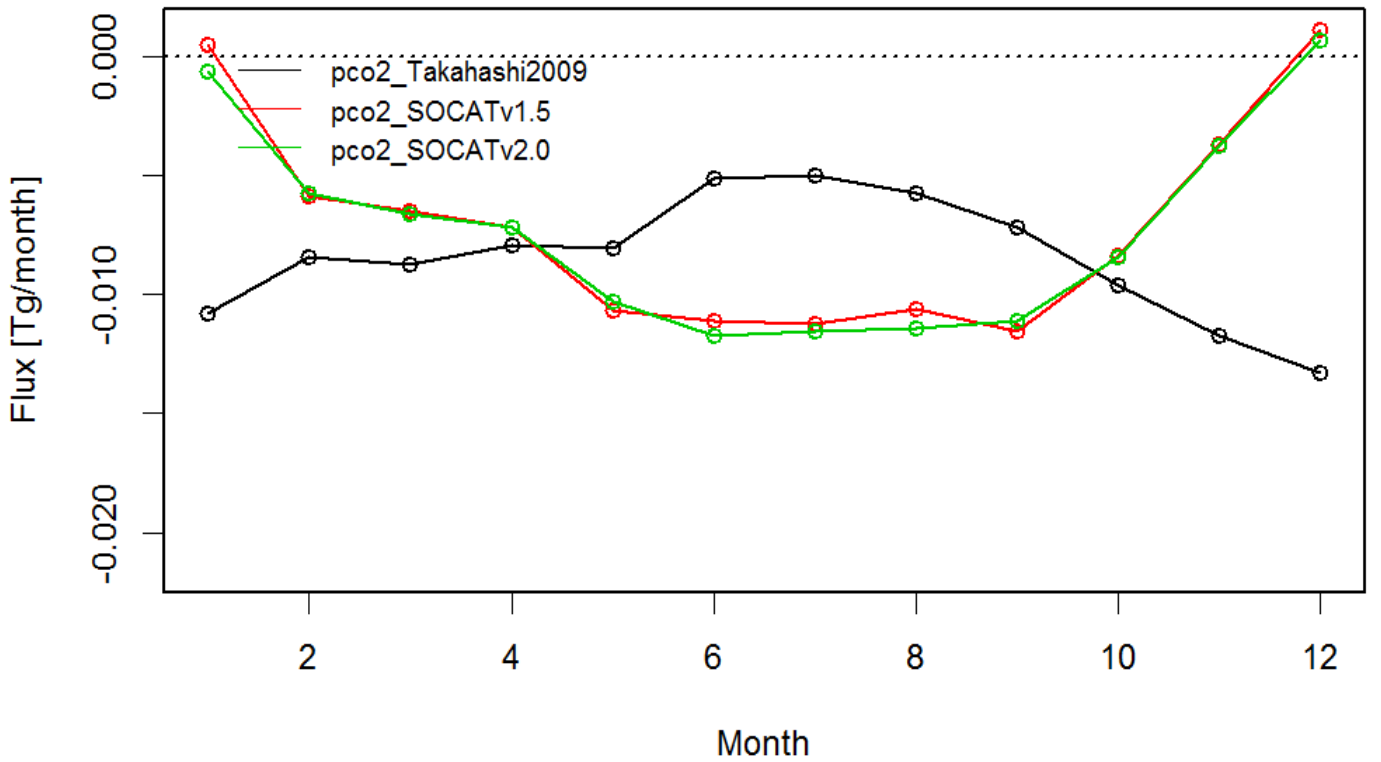
801
802

a)



803
804

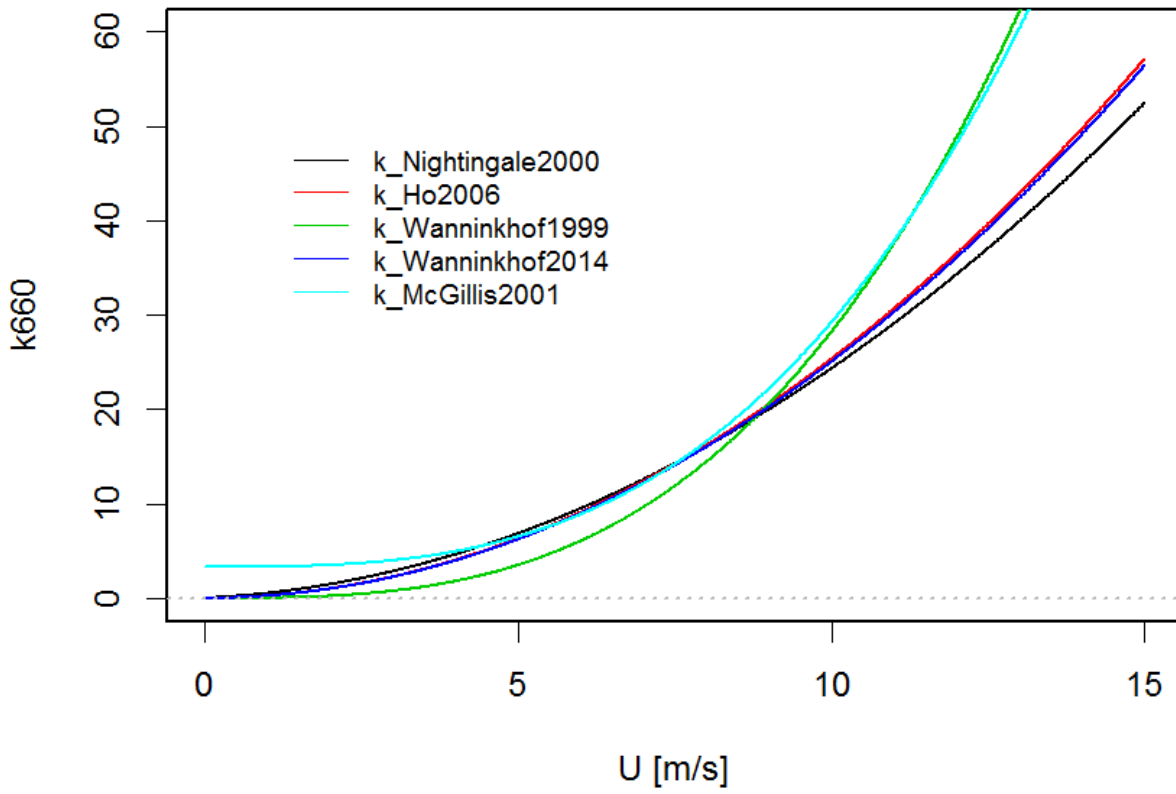
b)



805
806
807
808

Figure 8. Comparison of monthly values fluxes of air-sea CO₂ fluxes calculated with different $p\text{CO}_2$ climatologies (Takahashi et al. 2009, SOCAT v. 1.5 and 2.0) using the same k parameterization (Nightingale et al. 2000) in a) North Atlantic, b) European Arctic.

809
810



811
812 Figure 9. Different k660 parameterizations as a function of wind speed.